

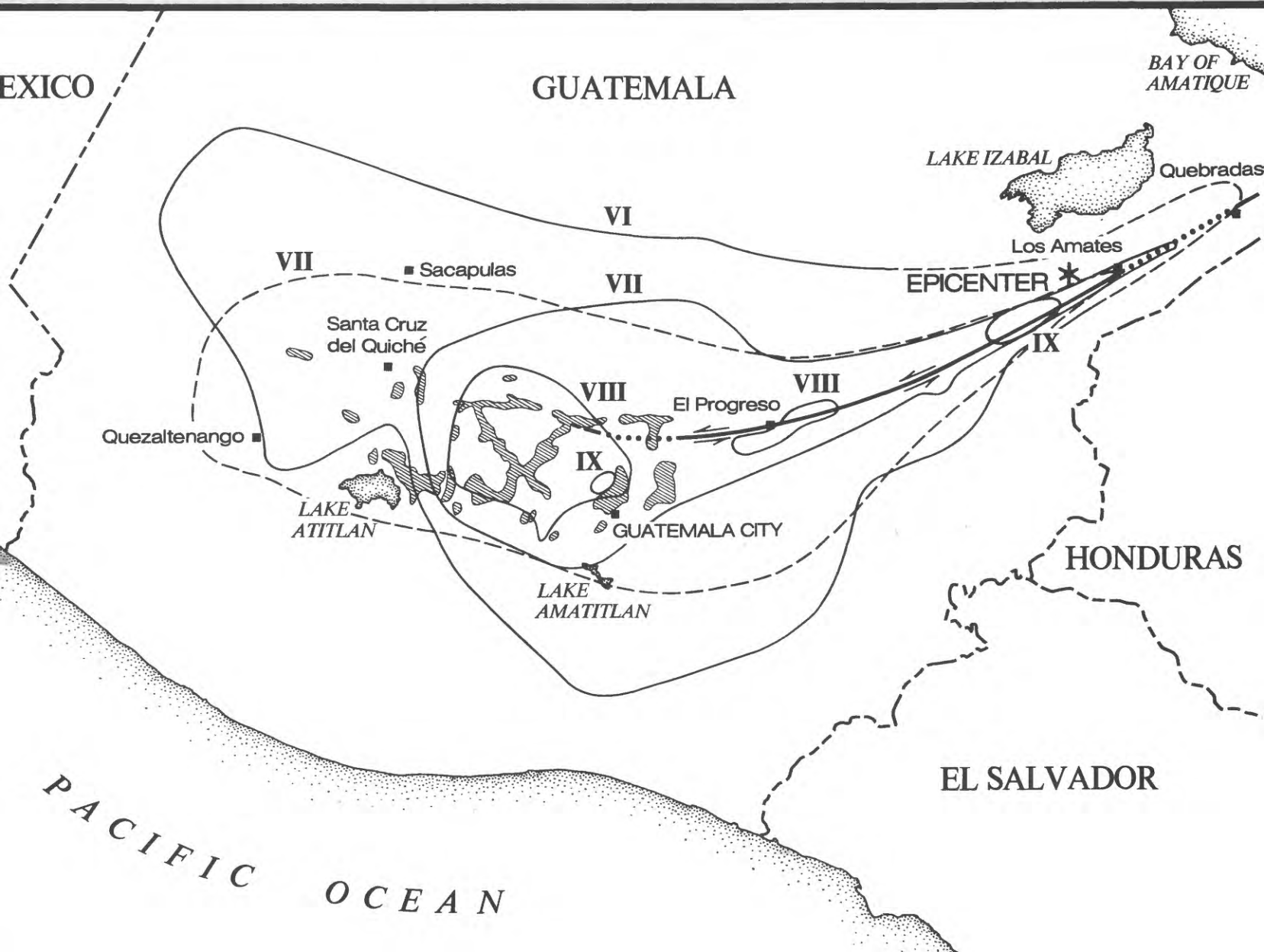
THE GUATEMALA EARTHQUAKE OF FEBRUARY 4, 1976

LANDSLIDES FROM THE FEBRUARY 4, 1976, GUATEMALA EARTHQUAKE

*Conducted in cooperation with
the Government of Guatemala,
under the auspices of the Agency
for International Development,
U.S. Department of State*



GEOLOGICAL SURVEY PROFESSIONAL PAPER 1204-A



Landslides from the February 4, 1976, Guatemala Earthquake

By EDWIN L. HARP, RAYMOND C. WILSON, *and*
GERALD F. WIECZOREK

THE GUATEMALA EARTHQUAKE OF FEBRUARY 4, 1976

GEOLOGICAL SURVEY PROFESSIONAL PAPER 1204-A

*Conducted in cooperation with the
Government of Guatemala, under the auspices of
the Agency for International Development,
U.S. Department of State*

*A description of the largest landslides,
a discussion of failure mechanisms, a
mapping of landslides throughout most of
the landslide-affected area, and a
mapping of landslide concentration in
the Guatemala City area*

UNITED STATES DEPARTMENT OF THE INTERIOR

JAMES G. WATT, *Secretary*

GEOLOGICAL SURVEY

Doyle G. Frederick, *Acting Director*

Library of Congress Cataloging in Publication Data

Harp, Edwin L.

Landslides from the February 4, 1976, Guatemala earthquake.

(The Guatemala earthquake of February 4, 1976)

(Geological Survey Professional Paper 1204-A)

Bibliography: p. 34

Supt. of Docs. no.: I 19.16

I. Landslides—Guatemala—Guatemala City region. I. Wilson, Raymond C., joint author.

II. Wiczorek, Gerald F., joint author. III. Title. IV. Series: Guatemala earthquake of February 4, 1976.

V. Series: United States Geological Survey Professional Paper 1204-A.

QE599.G9H37

551.3

80-607928

For sale by the Branch of Distribution, U.S. Geological Survey
Washington, D.C. 20404

CONTENTS

	Page		Page
Abstract	1	Large individual landslides	12
Introduction	1	Los Chocoyos	12
Investigation procedure	2	San José Poaquil	16
General damage from earthquake-induced landslides—impact on people, property, and lifelines	2	San Martín Jilotepeque	19
Predominant landslide types—characteristics and probable failure mechanisms	4	Estancia de la Virgen	22
Regional landslide distribution	8	Other large landslides	24
Factors affecting regional landslide distribution	8	Landslide concentration in the Guatemala City area	25
Seismic intensity	9	Factors affecting landslide concentration	28
Lithology	9	Lithology	28
Slope steepness	10	Fractures	30
Amplification of ground motion by topography	10	Topographic amplification	30
Regional fracture systems	12	Recommendations for reduction of seismically induced landslide hazard in Guatemala City	32
Preearthquake landslides	12	Summary	32
		References cited	34

ILLUSTRATIONS

	Page
PLATE 1. Seismically induced landslides from the February 4, 1976, Guatemala earthquake—eastern sector	In pocket
2. Seismically induced landslides from the February 4, 1976, Guatemala earthquake—western sector	In pocket
FIGURE 1. Map showing epicenter, fault rupture, and approximate limits of landslides of the February 4, 1976, Guatemala earthquake	3
2. Map showing areas of highest seismically induced landslide occurrence and Pleistocene pumice distribution in southwestern Guatemala	5
3. Sketch showing types of landslides generated by the February 4, 1976, Guatemala earthquake	6
4. Aerial photograph showing debris slides on slopes near Río Motagua	7
5-11. Photographs showing:	
5. Remains of house in Guatemala City that collapsed from landslides beneath it	7
6. Shallow debris slides	7
7. Typical seismically induced rock fall in pumice	8
8. Aerial view of rock falls in northern Guatemala City	8
9. High landslide concentration along slopes of Ríos Pixcayá and Xaltayá	10
10. Rock falls and debris slides due to topographic amplification of seismic ground motion	10
11. Rockfalls and debris slides on narrow ridge near Los Chocoyos	11
12. Diagram of theoretical seismic-ground-motion amplification by topography	11
13. Map of orthogonal lineament system in highlands west of Guatemala City	13
14. Aerial photograph of reactivated landslide along Río Cotzibal	14
15. Aerial photograph of preearthquake landslide complex at Laguneta del Tul	14
16. U-2 photograph of landslide at Los Chocoyos	15
17. Aerial photograph of landslide at Los Chocoyos	16
18-22. Photographs showing:	
18. Lake dammed behind landslide at Los Chocoyos	16
19. Stream-cut channel through landslide debris at Los Chocoyos	16
20. Lake level as of June 1976	16
21. Headwall scarp of landslide at Los Chocoyos	17
22. Los Chocoyos landslide debris and white pumice ridge along north margin	17

	Page
FIGURE 23. U-2 photograph of landslide 2 km northeast of San José Poaquil	18
24. Aerial photograph showing rotational slump/avalanche 2 km northeast of San José Poaquil	19
25-32. Photographs showing:	
25. Pumice and welded-tuff debris of landslides near San José Poaquil	19
26. Typical dark-gray welded-tuff fragment from San José Poaquil landslide mass	19
27. Headwall scarp of landslide near San José Poaquil	19
28. Intersection of lateral scarp and headwall scarp	20
29. Lateral and headwall scarps of San José Poaquil landslide	21
30. Landslide mass in zone 1 near headwall scarp	21
31. Highly deformed material in zone 2	21
32. Toe of San José Poaquil landslide	22
33. U-2 photograph of landslide 1 km southwest of San Martín Jilotepeque	23
34. Aerial photograph of lateral-spread/earthflow complex 1 km southwest of San Martín Jilotepeque	24
35. Aerial photograph of headwall scarp of San Martín Jilotepeque landslide	24
36. Photograph of inner and outer lateral shear ridges on north margin of earth-flow tongue	25
37. U-2 photograph of slump/avalanche near village of Estancia de la Virgen	26
38. Aerial photograph of slump/avalanche at Estancia de la Virgen, showing internal features	27
39. Aerial photograph of headwall scarp of landslide at Estancia de la Virgen	27
40. Photograph showing landslide toe	28
41. Aerial photograph showing extension fractures in headwall scarp	29
42. Aerial photograph showing landslide on Río Los Cubes	29
43. U-2 photograph of flow landslide north of Tecpán	29
44. Aerial photograph of slump/avalanche near Finca San Carlos	30
45. Aerial photograph of incipient slump near El Zarzal	30
46. Map of landslide concentration for the Guatemala City area	31
47. Diagram showing landslide dimensions and method of calculating landslide concentrations	32
48. Photograph showing headwall of Río Guacamaya barranco	33
49. Map of intensities and landslides from 1976 earthquake within the Guatemala City area	34
50. Aerial photograph of housing development in northern Guatemala City, showing extensive rock fall on end of narrow ridge	34

TABLE

	Page
TABLE 1. Large seismically induced landslides	4

LANDSLIDES FROM THE FEBRUARY 4, 1976, GUATEMALA EARTHQUAKE

By EDWIN L. HARP, RAYMOND C. WILSON, and GERALD F. WIECZOREK

ABSTRACT

The M (Richter magnitude) = 7.5 Guatemala earthquake of February 4, 1976, generated more than 10,000 landslides throughout an area of approximately 16,000 km². These landslides caused hundreds of fatalities as well as extensive property damage. Landslides disrupted both highways and the railroad system and thus severely hindered early rescue efforts. In Guatemala City, extensive property damage and loss of life were due to ground failure beneath dwellings built too close to the edges of steeply incised canyons.

We have recorded the distribution of landslides from this earthquake by mapping individual slides at a scale of 1:50,000 for most of the landslide-affected area, using high-altitude aerial photography. The highest density of landslides was in the highlands west of Guatemala City. The predominant types of earthquake-triggered landslides were rock falls and debris slides of less than 15,000 m³ volume; in addition to these smaller landslides, 11 large landslides had volumes of more than 100,000 m³. Several of these large landslides posed special hazards to people and property from lakes impounded by the landslide debris and from the ensuing floods that occurred upon breaching and rapid erosion of the debris.

The regional landslide distribution was observed to depend on five major factors: (1) seismic intensity; (2) lithology: 90 percent of all landslides were within Pleistocene pumice deposits; (3) slope steepness; (4) topographic amplification of seismic ground motion; and (5) regional fractures. The presence of preearthquake landslides had no apparent effect on the landslide distribution, and landslide concentration in the Guatemala City area does not correlate with local seismic-intensity data. The landslide concentration, examined at this scale, appears to be governed mainly by lithologic differences within the pumice deposits, preexisting fractures, and amplification of ground motion by topography—all factors related to site conditions.

INTRODUCTION

The $M=7.5$ Guatemala earthquake of February 4, 1976, generated at least 10,000 landslides that caused hundreds of fatalities as well as extensive property damage in the Guatemala City area. In response to a request by the Government of Guatemala, the U.S. Geological Survey sent scientists and engineers to study the effects of the earthquake. The purpose of this study, funded in part by the Agency for International Develop-

ment, U.S. Department of State, was to map the distribution of earthquake-induced landslides, to determine the mechanisms of their formation, and to lend technical assistance to the Guatemala Government in assessing the future hazard to people and property in areas where apparent landslide hazards remain. Another objective of our study was to depict the landslide distribution in the Guatemala City area in terms of zones of relative concentration, and to correlate these zones with geologic and geophysical parameters to assess the probability of a similar landslide distribution in future earthquakes.

Previous reconnaissance studies of the effects of major earthquakes have been largely concerned with damage to manmade structures, fault rupture, or seismologic parameters of the earthquake and its aftershocks. Although ground-failure effects account for many of the fatalities and much of the property damage in major earthquakes, relatively few postearthquake reports have mapped seismically induced landslides on a regional scale, described the different types of failures, or analyzed the seismic, geologic, and geotechnical parameters of the triggering process. Tuthill and Laird (1966) mapped large seismically induced rock-fall avalanches from the 1964 Alaska earthquake ($M=8.3$) in part of the Chugach Range. Plafker, Ericksen, and Concha (1971) presented a map showing landslide locations over most of the area affected by the 1970 Peru earthquake ($M=7.75$) and discussed the features and mechanisms of slope failure and debris transport in the catastrophic Huascarán rock-fall avalanche, which destroyed most of the town of Yungay. Morton (1971) prepared a map of landslide locations from the 1971 San Fernando, Calif., earthquake ($M=6.4$) on which he distinguished landslide types and documented their respective predominance.

In this report we describe and discuss the following topics: (1) the general damage resulting from seismically induced landslides; (2) the predominant landslide types, their areal distribution, and slope-failure mechanisms; (3) the regional distribution of seismically induced landslides and the factors that strongly influenced this distribution (see map of configurations and locations of earthquake-induced landslides in pls. 1, 2); (4) the characteristics and failure mechanisms of the four largest landslides and the hazards imposed by each slide; (5) the landslide distribution within the Guatemala City area, in the form of a landslide concentration map, and the major factors influencing this distribution; and (6) the outlook for Guatemala City in terms of landslide susceptibility in future earthquakes.

INVESTIGATION PROCEDURE

The distribution and types of seismically induced landslides were determined from aerial photographs coupled with aerial reconnaissance and ground-based fieldwork. Photointerpretation and photomapping of both postearthquake and obvious preearthquake landslides were performed using U-2 photography taken on February 13, 1976, by the U.S. Air Force under contract to the Office of Foreign Disaster Assistance of the Agency for International Development, U.S. Department of State. Though taken from an altitude of approximately 21 km, the photographs have a resolution of about 1 m and afforded stereoscopic coverage of the entire area in which earthquake-induced landslides occurred.

Landslides in the affected area were mapped on 1:50,000-scale topographic base maps, and in the Guatemala City area on a 1:12,500-scale topographic base map; all base maps were provided by the Instituto Geográfico Nacional de Guatemala. Fieldwork was done to check the accuracy of photomapping and to investigate landslide characteristics and mechanisms during a period of two weeks in April and two weeks in June 1976. In addition to the general reconnaissance effort, we spent several days at each of the sites of the four largest landslides.

Acknowledgments.—We acknowledge the assistance both of Oscar Salazar and Sam Bonis of the Instituto Geográfico Nacional, in providing logistic support for the field investigations; and of the staff of the Regional Office, Central America and Panama, of the U.S. Agency for International Development, for arrangement of ground and air transportation. We also thank George Plafker for sharing knowledge of regional structure and stratigraphy and information regarding landslide-associated incidents that took place within a week after the earthquake. We gratefully acknowledge the help of

Joshua Rosenfeld, who shared with us his knowledge of the local geology and provided technical translation during part of our fieldwork. We thank Robert Fleming and David Varnes, who provided technical assistance during part of the fieldwork and reviewed the manuscript, and David McCulloch for his comments and critical review of the manuscript. We thank the Guatemalan people, both private citizens and public officials, who enthusiastically provided helpful information and related their personal experiences of the earthquake and accompanying landslides; interviews with them contributed much to our interpretation of landslide behavior during this earthquake.

GENERAL DAMAGE FROM EARTHQUAKE-INDUCED LANDSLIDES— IMPACT ON PEOPLE, PROPERTY, AND LIFELINES

The epicenter of the February 4, 1976, Guatemala earthquake was within the Motagua fault zone near Los Amates, about 157 km northeast of Guatemala City (Person and others, 1976). The earthquake triggered landslides over an area of approximately 16,000 km² that extends from near Quebradas on the east to Quezaltenango on the west and from near Lago de Amatitlán on the south to near Sacapulas on the north. This area is only a few kilometers wide in the epicentral area but expands to the southwest, where it widens to about 80 km in the highlands. The approximate limits within which landslides occurred are shown on the index map (fig. 1).

Most landslides occurred on the steep slopes of the rugged Guatemalan highlands, and were particularly heavily concentrated along the canyons of the Ríos Pixcayá, Motagua, Las Vacas, and Los Chocoyos (fig. 2). Relatively few landslides occurred near the epicenter or along the valley of the Río Motagua northeast of Guatemala City.

The predominant types of landslides¹ induced by this earthquake (fig. 3) were rock falls and debris slides of less than 15,000 m³ volume. In some areas, however, landslides coalesced so extensively that as much as 80 percent of slopes were denuded (fig. 4).

In addition to the thousands of small to moderate-size (less than 15,000 m³) rock falls and debris slides, 11 large landslides had volumes of over 100,000 m³. Several of these large landslides blocked stream drainages and thus posed an additional hazard from flooding. The four

¹As used throughout this report, the term "landslide" specifically excludes ground failure due to liquefaction, such as lateral-spread failure, unless otherwise stated.

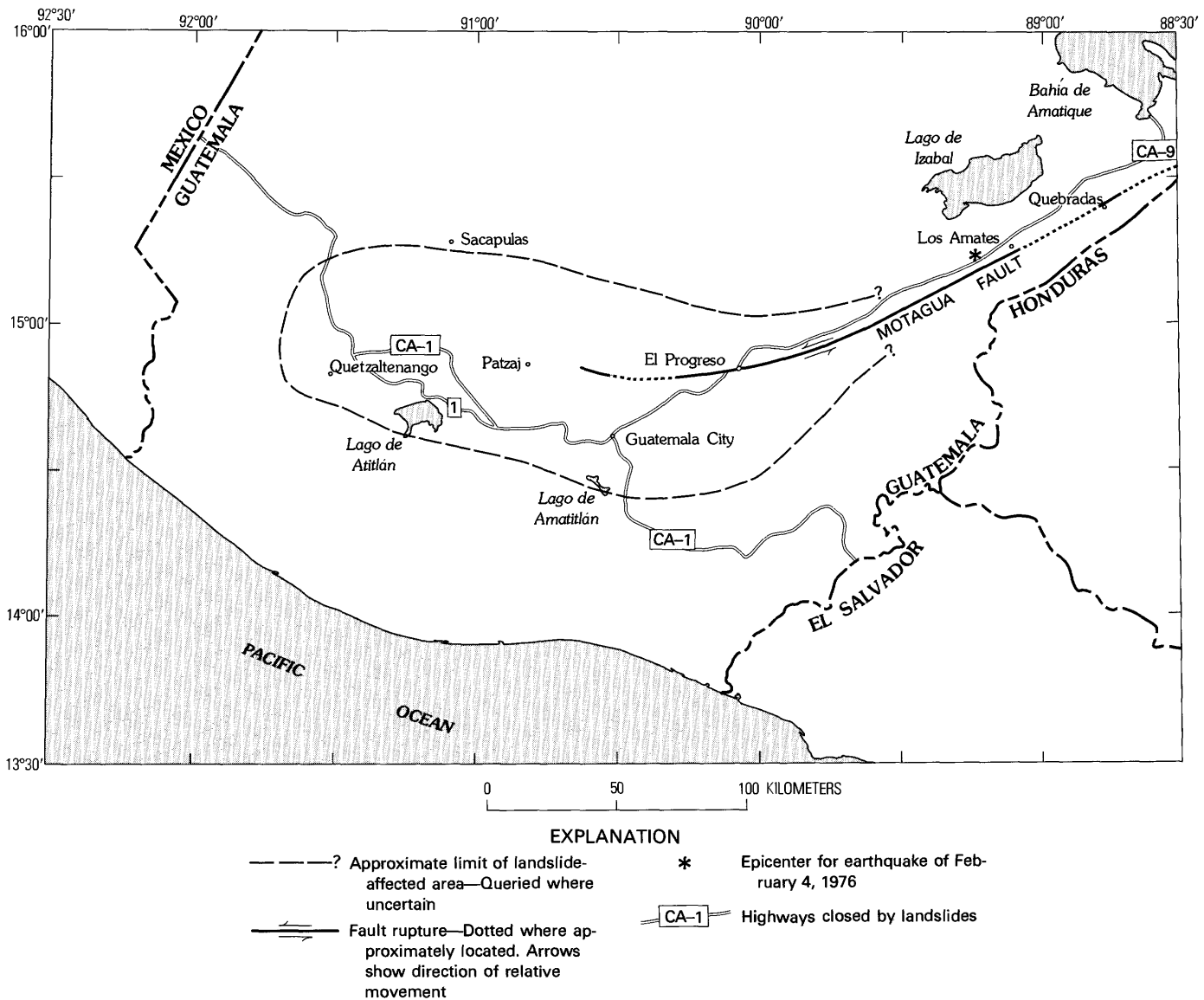


FIGURE 1.—Epicenter (Person and others, 1976), fault rupture (Plafker and others, 1976), and approximate limits of landslide-affected area in the February 4, 1976, Guatemala earthquake, and highways closed by landslides.

largest landslides—near Los Chocoyos, San José Poaquil, San Martín Jilotepeque, and Estancia de la Virgen—are discussed in detail in the section entitled “Large Individual Landslides” (see table 1).

There were 37 reported deaths as a direct result of landslides in the highlands west of Guatemala City, all related to 3 of the largest landslides. A few fatalities were reported from the breach of landslide-dammed lakes (George Plafker, oral commun., 1976); other fatalities were probably caused by landslides that occurred in isolated areas of the highlands but were not reported. Although the number of fatalities due to landslides is small compared to the number of casualties from col-

lapsed adobe dwellings, landslide-related fatalities could have been much more numerous if the areas of highest landslide density or of the largest deep-seated landslides had been on canyon slopes within a heavily populated area.

Landslides disrupted major highways and the national railroad system. The Atlantic Highway (CA9, fig. 1) was blocked by landslides at numerous points between Guatemala City and El Progreso; the Pan American Highway (CA1) was blocked by landslides in the Mixco area west of Guatemala City and near Tecpán; and Highway 10 was buried by a massive slide at Los Chocoyos. These highway blockages seriously hindered

TABLE 1.—Large seismically induced landslides

Site ¹	Locality	Rock type	Failure type	Estimated volume [10 ⁶ m ³]	Average slope ²	Remarks
1	Los Chocoyos - - - - -	Pumice, consisting of tephra H and H ash-flow tuff of Koch and McLean (1975).	Block slide/rock-fall avalanche	0.75-1.0	27°	Failure sudden and catastrophic; 7 people killed.
2	San José Poaquil - - -	Dark-gray welded tuff with thin irregular cap of pumice.	Complex block slide/rotational slump grading into rock-fall avalanche near toe.	3.5	19°	Little effect on lives and property. Lake breached on June 27, 1976.
3	San Martín Jilotepeque	Pumice, probably H ash-flow tuff of Koch and McLean (1975).	Complex rotational slump in head-wall; long, tongue-shaped north one-third resembled an earthflow; south two-thirds was an incipient rotational-slump lateral spread extensively fractured throughout.	1.0	11°	Destroyed 14 houses and killed 17 people; dammed Río Quemayá. Breach of lake, which drowned several people, may have been liquefaction induced.
4	Estancia de la Virgen	Tertiary andesitic volcanic rocks.	Rotational slump/rock-fall avalanche	6.0	23°	Dammed Río Pixcayá; 13 people killed in slide.
5 ²	Río Polima - - - - -	Tertiary andesitic volcanic rocks overlain by pumice.	Block slides	<.2	27°	Created a small lake about 200 m long and about 2 m deep (June 1976).
6 ²	Río Naranjo - - - - -	Pumice	Disintegrating rotational slump	<.3	---	No impounded water behind slide as of June 1976.
7 ²	Río Blanco - - - - -	Tertiary andesitic volcanic rocks overlain by pumice.	Complex coalescing rock-fall avalanche	<.2	26°	Small lakes impounded behind rocky debris had drained by June 1976.
8 ²	Río Ruyalché - - - - -	Tertiary andesitic volcanic rocks overlain by pumice.	Rotational slump	<.5	15°	No lake behind slide mass as of June 1976.
9 ²	Río Cotzibal - - - - -	Tertiary andesitic volcanic rocks.	Rotational slump	.3	15°	River only partly blocked; incipient slide.
10	Río Teocinte - - - - -	Tertiary andesitic volcanic rocks.	Rotational slump/rock-fall avalanche	.3-5	29°	Small lake dammed but drained as of June 1976.
11 ²	Río Los Cubes - - - - -	Paleozoic(?) metamorphic rocks	Block slide/avalanche	<.1	28°	Lake about 200 m long and about 3-4 m deep, draining through slide material (June 1976).

¹See plates 1 and 2 for locations.

²Landslides at these sites were not visited on the ground, but low-altitude aerial observations were made, and numerous photographs were taken. Volume estimates for these landslides are extremely rough, and for others are based on field and photographic measurements.

³Preearthquake topography.

rescue and relief efforts in the severely damaged towns and villages of the Guatemalan highlands. The railroad between Guatemala City and Puerto Barrios, the Caribbean port, was also blocked in more than 30 places (Chang, engineer, Ferrocarriles de Guatemala, written commun., 1976).

The most extensive property damage and loss of life from landsliding during the 1976 earthquake were in Guatemala City. The city is built on a plateau along the Continental Divide; this plateau is deeply incised by several streams that form a network of steep narrow canyons (locally called "barrancos") as deep as 100 m. The plateau is underlain by Pleistocene pumice deposits more than 100 m thick (Koch and McLean, 1975), a brittle material with extremely low tensile strength. The interlocking texture of the pumice, however, provides sufficient shear strength to support nearly vertical slopes 100 m high.

The extent of property damage or loss of life in the

Guatemala City area as a direct result of landsliding is not precisely known, but a conservative estimate would be approximately 500 dwellings damaged and at least 200 deaths. Most houses damaged by landslides were within 5 m of the canyon rims; these houses were either undermined by failure of the adjacent slopes or deformed by fissures that became incipient landslide scarps. A few neighborhoods on the slopes or bottoms of the barrancos were damaged by falling debris from slope failures (fig. 5).

PREDOMINANT LANDSLIDE TYPES— CHARACTERISTICS AND PROBABLE FAILURE MECHANISMS

Rock falls² and debris slides² were by far the most common types of landslides induced by the earthquake.

²Landslides are classified according to the nomenclature of Varnes (1978).

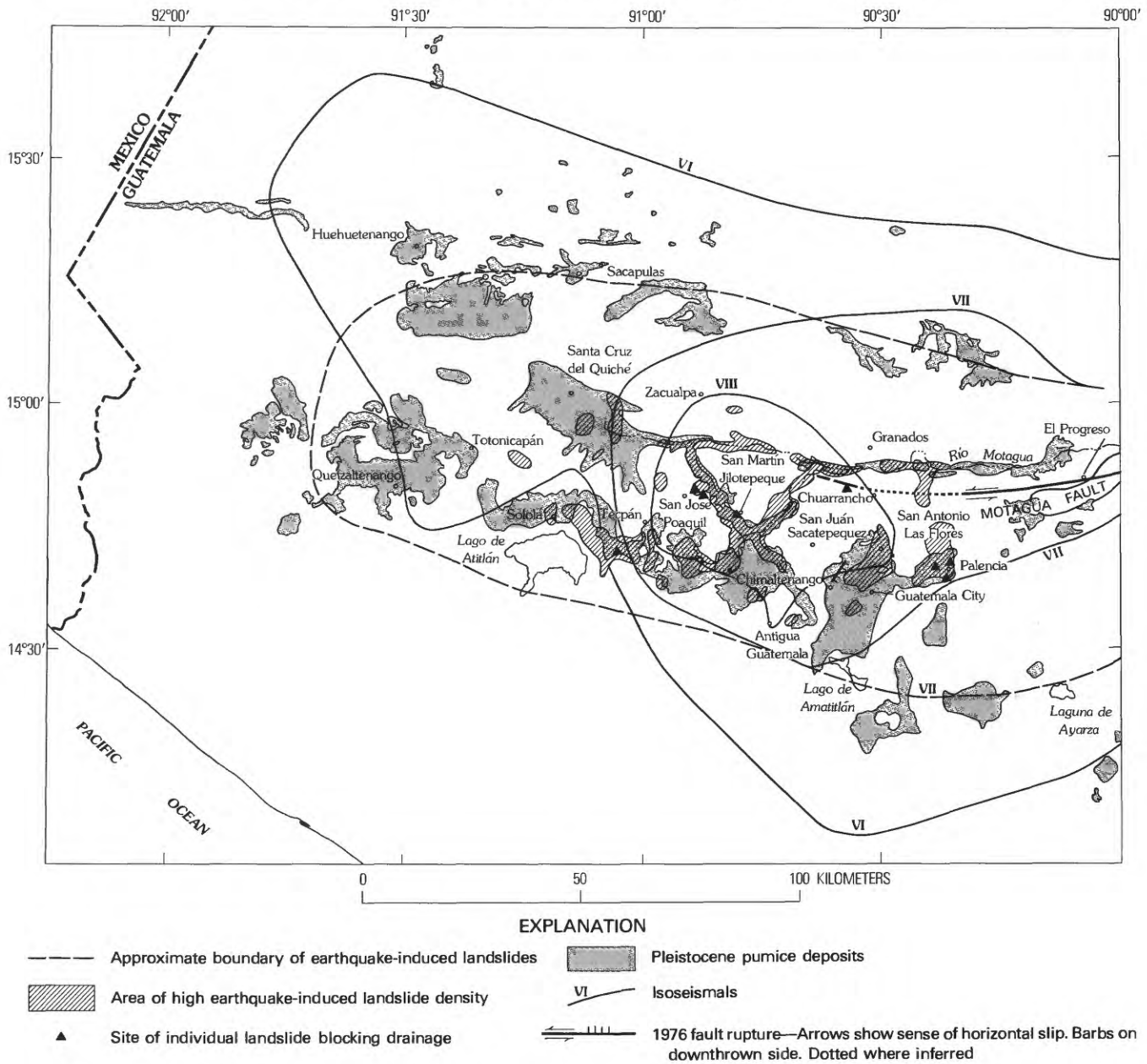


FIGURE 2.—Southwestern Guatemala, showing areas of high density of earthquake-induced landslides, distribution of Pleistocene pumice deposits (Bonis and others, 1970; Koch and McLean, 1975), isoseismals (Espinosa and others, 1976), fault rupture (Plafker and others, 1976), and approximate limits of landslide-affected area.

More than 90 percent of these rock falls and debris slides were within Pleistocene pumice deposits or their residual soils, and most of the landslides were relatively small (less than 15,000 m³ volume). Rock falls and debris slides had the highest overall impact of all landslide types on people and property because of their widespread occurrence and extremely high incidence in many areas.

Debris slides were most abundant in areas where thin soil (thinner than 0.6 m) is formed on pumice bedrock. This soil consists of medium-grained to coarse sand-size

fragments of weathered pumice and includes small amounts of clay. At the time of the earthquake, the soil was dry. Failure occurred by decoupling at or near the soil/bedrock interface, and subsequent movement took place by sliding along this discontinuity. Where the debris was partially held together by thin topsoil and vegetation, soil debris did not slide more than a few meters. However, most debris slides disaggregated into sand-size fragments and formed small debris avalanches (fig. 6).

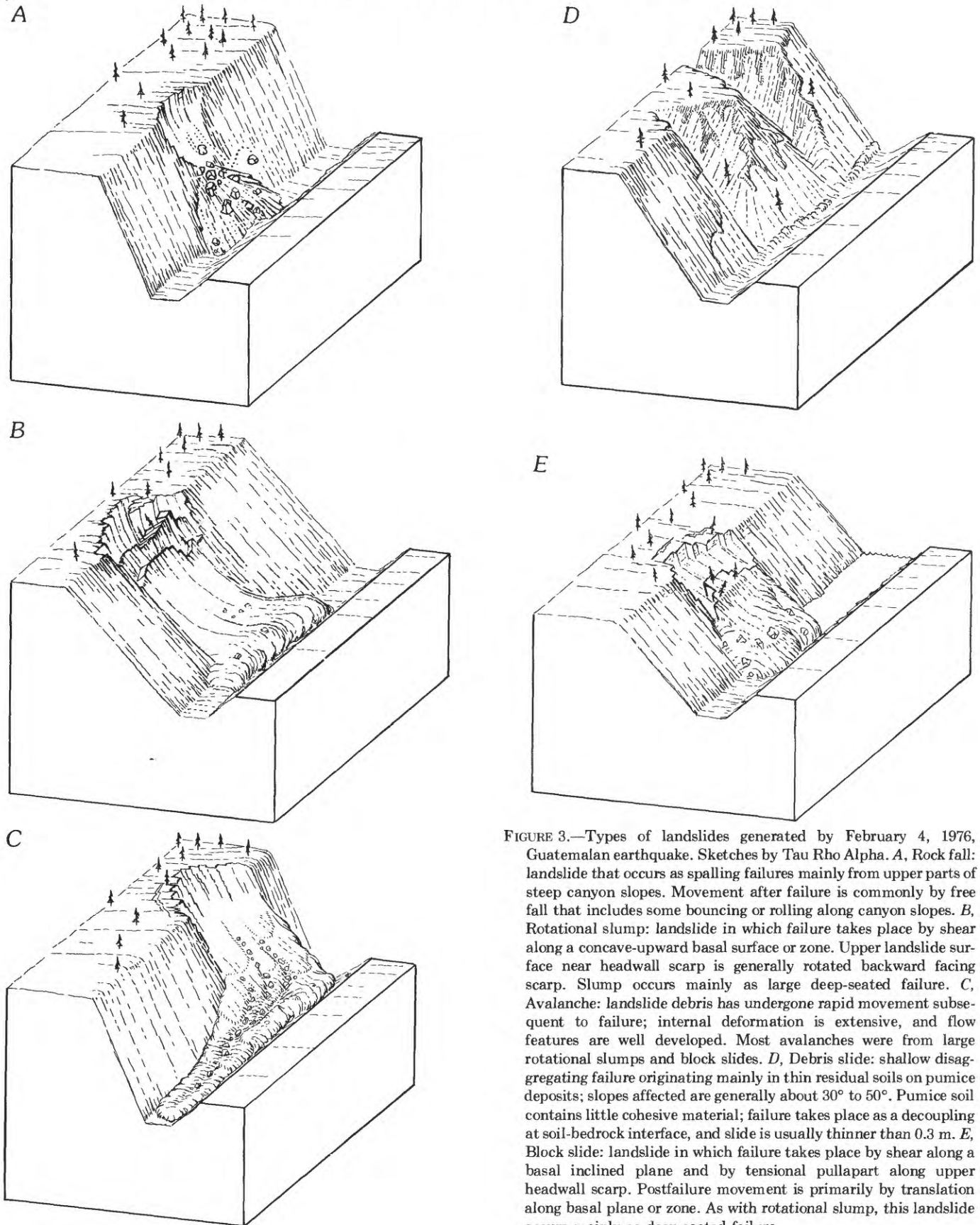


FIGURE 3.—Types of landslides generated by February 4, 1976, Guatemalan earthquake. Sketches by Tau Rho Alpha. *A*, Rock fall: landslide that occurs as spalling failures mainly from upper parts of steep canyon slopes. Movement after failure is commonly by free fall that includes some bouncing or rolling along canyon slopes. *B*, Rotational slump: landslide in which failure takes place by shear along a concave-upward basal surface or zone. Upper landslide surface near headwall scarp is generally rotated backward facing scarp. Slump occurs mainly as large deep-seated failure. *C*, Avalanche: landslide debris has undergone rapid movement subsequent to failure; internal deformation is extensive, and flow features are well developed. Most avalanches were from large rotational slumps and block slides. *D*, Debris slide: shallow disaggregating failure originating mainly in thin residual soils on pumice deposits; slopes affected are generally about 30° to 50° . Pumice soil contains little cohesive material; failure takes place as a decoupling at soil-bedrock interface, and slide is usually thinner than 0.3 m. *E*, Block slide: landslide in which failure takes place by shear along a basal inclined plane and by tensional pullapart along upper headwall scarp. Postfailure movement is primarily by translation along basal plane or zone. As with rotational slump, this landslide occurs mainly as deep-seated failure.

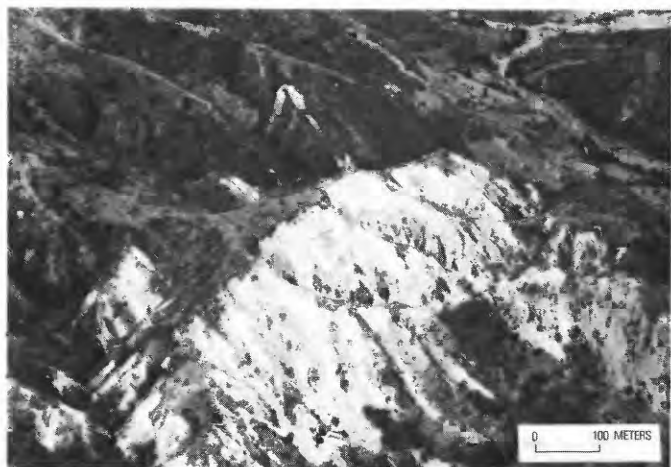


FIGURE 4.—Pumice slopes near Río Motagua, about 25 km north of Guatemala City, on which extensive failures and coalescence of debris slides occurred. Most slides are shallow, typically thinner than 1 m.



FIGURE 5.—Remains of house in northern Guatemala City, built too close to canyon margin. House collapsed owing to rock-fall failure beneath foundation from an aftershock shortly after main shock.

The effect of two rainy seasons (1976 and 1977) on the areas of heavy debris slides since the earthquake has been to strip even more soil cover from the disturbed slopes. Apparently, once the first earthquake-induced debris slides formed and breached the soil cover, the slopes became exceptionally vulnerable to erosion. The accelerated debris-slide occurrence from rainfall erosion since the earthquake may well continue until many slopes are completely devoid of soil.

The mechanism of rock-fall formation within the pumice deposits appears to have been tensile fracture resulting from interaction of seismic waves with the free faces of the canyon walls. The average tensile strength of the pumice is probably less than 35 kilopascals (KPa), an estimate based on our field observations that boulder-



FIGURE 6.—Shallow debris slides in pumice slopes along Río Motagua; depth of failure averages no more than 0.6 m. Climate in this area of river drainage is arid, and soils formed on pumice here are thin, sandy, and low in clay content.

size pieces of pumice bedrock, though massive in outward appearance, could be easily broken apart and disaggregated by hand. Our attempts to collect undisturbed samples of the pumice were largely unsuccessful. The ability of the pumice deposits to stand as vertical cliffs and yet to undergo brittle fracture from seismic shaking appears to derive from mechanical strength imparted by cohesion due to the interlocking fabric of the highly angular pumice clasts.

Rock falls were most common where nearly vertical slices of pumice broke away from the upper parts of canyon slopes, commonly near the slope crest. In many places the rock-fall scarp is bounded by nearly vertical cracks. These rock falls were generally thinner than 6 m. Incipient failures as thick as 15 to 30 m were observed in some places where multiple scarps were created near the plateau margins and where one or more thin slices of pumice had fallen, leaving additional blocks on the verge of failure, whose boundaries were defined by extension fractures in the flat plateau surface. As in the debris slides, rock-fall material was generally dry at the time of the earthquake; a typical rock-fall scarp has an irregular more or less concave outward surface (figs. 7, 8).

Rock falls on slopes in rock types other than pumice overall morphologically resembled rock falls in pumice, the primary difference being the influence of preearthquake fractures or joint surfaces on the formation of failure scarps. Thus, weathered andesite, a common rock type throughout the Guatemalan highlands, failed mainly along preexisting fractures and not through intact rock, as was common for rock falls within pumice. We attribute this difference in mode of failure to the relatively low tensile strength of the pumice as compared with most other rocks. Furthermore, the landslide debris



FIGURE 7.—Typical seismically induced rock fall in pumice deposits along canyon margin near Puente Belize in Guatemala City. Failure is no thicker than 1 to 2 m (normal to canyon face) and is overall concave outward. Unslickensided rock-fall scarp indicates no shear deformation. Such failures were probably caused by tensile spalling, possibly from seismic-wave reflection at free faces.

from nonpumice rocks was coarser on the average than that from pumice rock falls—a reflection of the fracture spacing common in the Tertiary volcanic rocks, as compared with the primary sand- and gravel-size detrital particles into which much of the pumice disaggregated upon failure. The different rock types and their influence on landslide distribution are discussed in the section entitled “Factors Affecting Regional Landslide Distribution.”

The rock falls and debris slides in the 1976 Guatemala earthquake were similar to the seismically induced failures in many other large earthquakes (Keefer and others, 1978). Plafker, Ericksen, and Concha (1971) described rock falls and debris slides from the 1970 Peru earthquake ($M=7.75$) in several rock types, among which poorly consolidated valley fill, pyroclastic deposits, and weathered granodiorite were specifically mentioned. Weischet (1963) indicated that slopes of volcanic pumiceous tuff failed extensively as rock falls and debris slides in the 1960 Chilean earthquake



FIGURE 8.—View southward of extensive rock fall on canyon slopes just west of Finca La Verbena in Guatemala City. Rock falls left light scarps (arrows) in pumice cliffs and debris in canyon bottom.

($M=8.4$), but that much weathered granite and many other plutonic rocks also failed. Wright and Mella (1963) described the soils near Lago de Rupanco in Chile, made up of successive layers of volcanic ash and scoriaceous gravel that include intervening layers of weathered allophane-rich andesitic volcanic ash; this soil was extremely susceptible to debris slides and debris flows during the 1960 earthquake.

REGIONAL LANDSLIDE DISTRIBUTION

The accompanying maps (pls. 1, 2) show the locations of individual landslides from this earthquake and also of those preearthquake landslides that could be detected from U-2 photography. In several areas where slides were so concentrated that individual landslides could not be mapped at this scale (1:50,000), the information has been generalized so that boundaries reflect the areas of highest landslide density. Most landslides were mapped individually, and extensive field and photographic checking has shown the maps to indicate landslide locations and morphology accurately in almost all the landslide-affected region. A few areas on the fringes to the north and east in which landslides were relatively sparse have been omitted for simplicity.

FACTORS AFFECTING REGIONAL LANDSLIDE DISTRIBUTION

The regional landslide distribution from the 1976 Guatemala earthquake appears to be influenced by five

main factors: (1) seismic intensity, (2) lithology, (3) slope steepness, (4) topographic amplification of ground motion, and (5) regional fractures. Preearthquake landslides were found to have been reactivated little, if at all, during the earthquake.

SEISMIC INTENSITY

Noncoincidence of the epicenter with the areas of high landslide density far to the southwest (figs. 1, 2) is partly explained by the fact that shaking intensities were highest not in the epicentral region but in the highlands to the southwest. Espinosa, Husid, and Quesada (1976) have established that most of the energy of the earthquake was directed southwestward from the epicenter because of a westward-propagating source.

A comparison of our map of the areas of highest landslide density with the isoseismal map by Espinosa, Husid, and Quesada indicates that landslides occurred mostly within the modified Mercalli intensity (MMI) VI contour and that areas of high landslide density are largely within the MMI VII isoseismal (fig. 2). The MMI scale assigns a high seismic intensity to areas with pronounced ground failures, and areas of heavy landsliding generally receive a scale value of X (Wood and Neumann, 1931). Espinosa, Husid, and Quesada based their intensity survey largely on the degree of shaking damage to adobe dwellings and excluded landslides and other ground failures as secondary effects of seismic shaking. They also noted that adobe houses were relatively undamaged in several areas of heavy landslide activity and concluded that "landsliding implies intensity X, but undamaged adobe houses suggest much lower intensities" (Espinosa and others, 1976, p. 53). Our field observations of the degree of structural damage in many landslide-affected areas suggest that the threshold shaking intensity for triggering landslides in the most susceptible localities corresponded to an MMI of VI.

LITHOLOGY

Approximately 90 percent of the seismically induced landslides occurred within Pleistocene pumice deposits, about 10 percent in Tertiary volcanic rocks, and less than 1 percent in Cretaceous limestone and Paleozoic metamorphic rocks. The pumice deposits crop out over approximately 20 percent of the area of the southwestern highlands; volcanic rocks of Tertiary age (predominantly andesite) account for most other outcrops.

The Pleistocene pumice deposits consist of 26 air-fall tephra units, 4 sequences of ash-flow tuff, and 4 fluviolacustrine units (Koch and McLean, 1975). The tephra units, which are well sorted and contain angular pumice clasts, are commonly a few centimeters to

several meters thick. The ash-flow tuff units are poorly sorted and contain lapilli and bomb-size pumice and lithic fragments in a matrix of fine to coarse ash, pumice, and lithic fragments; the units range from about 1 to 100 m in thickness. The fluviolacustrine units are composed of well-stratified pumiceous ash and rounded gravel-size pumice. The pumice deposits, which all derive from episodes of explosive volcanic activity during Pleistocene time, accumulated in greatest thicknesses along river valleys and other topographic lows. The H ash-flow tuff of Koch and McLean (1975), the most extensive of the pumice units, is about 90 m thick along the Río Los Chocoyos (Koch and McLean, 1975).

The pumice deposits are not welded or extensively cemented but have undergone some compaction under their own weight. Thus the pumice has little cohesive strength and derives most of its shear strength and ability to support steep slopes under nonseismic conditions from a high coefficient of friction due to the angularity and interlocking fabric of individual particles. The comparatively low tensile strength of the pumice is probably the key factor making it especially susceptible to seismically induced failure.

As discussed above, most landslides within the pumice deposits were shallow rock falls and debris slides. Rock falls in pumice were the most uniformly distributed of all landslide types; debris slides, however, were heavily concentrated along the Río Motagua and along several other river-valley slopes immediately to the south. Debris slides show a well-defined gradational increase in incidence from south to north across the landslide-affected region. The number of debris slides increases from a few scattered near Guatemala City northward, until their density reaches several hundred per 100 m of horizontal slope length in areas where thin granular soil is formed on pumice slopes near the Río Motagua. This northward increase in debris-slide density parallels a variation in the soil thickness on pumice deposits. Near Guatemala City, soil commonly is 1 m thick or thicker, whereas to the north along the Río Las Vacas, the pumice soil thins rapidly to less than 0.5 m within a horizontal distance of 10 km.

The Tertiary volcanic rocks consist of acidic to basic breccia and flows; andesitic rocks predominate. Common landslide types in these rocks were rock falls and debris slides, and included seven large block slides and rotational slumps. The Tertiary volcanic rocks were much less susceptible to rock falls and debris slides than the pumice deposits, although most of the large landslides (table 1) occurred within the Tertiary rocks.

Within the Tertiary volcanic rocks, weathered and highly fractured slopes were most susceptible to rock falls. For example, steep slopes of rock-fall-prone andesite just west of Sololá contained networks of frac-

tures or joints spaced less than 0.3 m apart. For many months after the earthquake, these canyon slopes continued to slough cobble-size fragments onto the canyon floor below. In contrast, on the road between Sololá and Lago de Atitlán, unweathered andesite containing relatively few fractures produced correspondingly few rock falls.

About 1 percent of the landslides were in Cretaceous limestone and Paleozoic metamorphic rocks; rock falls, debris slides, and rotational slumps were the predominant landslide types. The highest landslide densities in the limestone were in roadcuts along the Atlantic Highway from Guatemala City toward El Progreso. The relatively small number of failures in these rocks compared with the Tertiary volcanic rocks may not have been due to any significant difference in susceptibility but rather to the fact that there are fewer outcrops of limestone and metamorphic rocks within the areas of highest seismic intensities (MMI VII-IX).

SLOPE STEEPNESS

Topography was a key factor in controlling the location and extent of landslides in all affected areas and in all rock and soil types. Without exception, rock falls occurred on steep (generally steeper than 50°) canyon slopes and ridges, and generally originated in the upper parts of slopes. On gentler (approximately 25° - 30°) slopes, thin granular soil of weathered pumice formed disintegrating debris slides. In a few areas, rock falls and debris slides commonly occurred on different parts of the same slopes; rock falls were on the steepest sections, and debris slides on the sections with gentler than 30° slope. Because most of the pumice deposits erode to statically stable steep cliffs, commonly 30 to 50 m high, these cliffs present one of the most seismically unstable situations in nature. Along the Ríos Pixcayá, Motagua, Los Chocoyos, and Las Vacas, where the incidence of rock falls and debris slides was particularly high, these slides left hundreds of square kilometers of steep slopes in conditions similar to those shown in figure 9.

AMPLIFICATION OF GROUND MOTION BY TOPOGRAPHY

Topographic amplification of seismic ground motion appears to have been another important factor affecting the distribution of landslides. Local concentrations of landslides indicate that the primary sites of seismic shaking in the canyon terrain were at pronounced topographic convexities. Rock falls and debris slides were particularly numerous along ridge crests and narrow promontories (figs. 10, 11); exposed bedrock in the landslide scarps on these slopes indicates that rock frac-



FIGURE 9.—View southeastward along junction of Ríos Pixcayá and Xaltayá, showing high density of rock falls and debris slides typical of steep pumice slopes in this area.



FIGURE 10.—Effects of apparent topographic amplification of seismic ground motion in concentrating rock falls and debris slides on narrow ridges, such as this ridge near Los Chocoyos. Failures were generally shallow; some shrubs and a few trees (arrows) remain on slope.

turing due to seismic shaking was especially severe. Similar effects in the 1971 San Fernando, Calif., earthquake were described by Nason (1971), in the 1968 Borrego Mountain earthquake by Castle and Youd (1972), and in the 1957 Daly City, Calif., earthquake by Bonilla (1959).

Wong and Jennings (1975) have investigated the effects of canyon topography on strong ground motion by numerical methods. They studied shear (*SH*) waves at several selected frequencies of steady-state harmonic



FIGURE 11.—Narrow ridge near Los Chocoyos, laid bare by concentrated rock falls and debris slides.

motion and at various incidence angles to a surface approximating the topography of Pacoima Canyon in southern California (fig. 12), in an attempt to simulate the Pacoima strong-motion record from the 1971 San Fernando earthquake. Their calculations indicate that the amplification trends depend on the angle of incidence of the incoming waves, on their frequency, and on the geometry of the reflecting surface. Their results show that the greatest amplifications are for nearly horizontal waves with wavelengths equal to or smaller than the canyon dimensions (distance between canyon walls), especially at the points of most pronounced slope convexities.

A uniform half-space produces an amplification factor of 2 because of reflection and constructive interference of both the incoming and reflected waves. An irregular surface can produce greater amplifications as well as reduction of wave motion at different points because of focusing of the waves at convexities and their dispersion at concavities. In the calculations of Wong and Jennings, amplifications by a factor of more than 6 were obtained at the points of greatest convexity; conversely, concavities decreased wave amplitudes. A wave reflected from a near canyon wall would be amplified, whereas one reflected from the far wall would be reduced by shielding. Amplification of ground motion at wavelengths greater than the canyon dimensions is little above that of a featureless half-space.

The typical relation of rock falls and debris slides to canyon-slope geometries in Guatemala agrees strikingly well with the patterns of amplification of ground motion predicted by the model of Wong and Jennings. Thus, we infer that a high percentage of the rock falls and debris slides in the 1976 Guatemala earthquake resulted from high dynamic stresses imposed by the amplification of seismic waves by the existing canyon topography. This

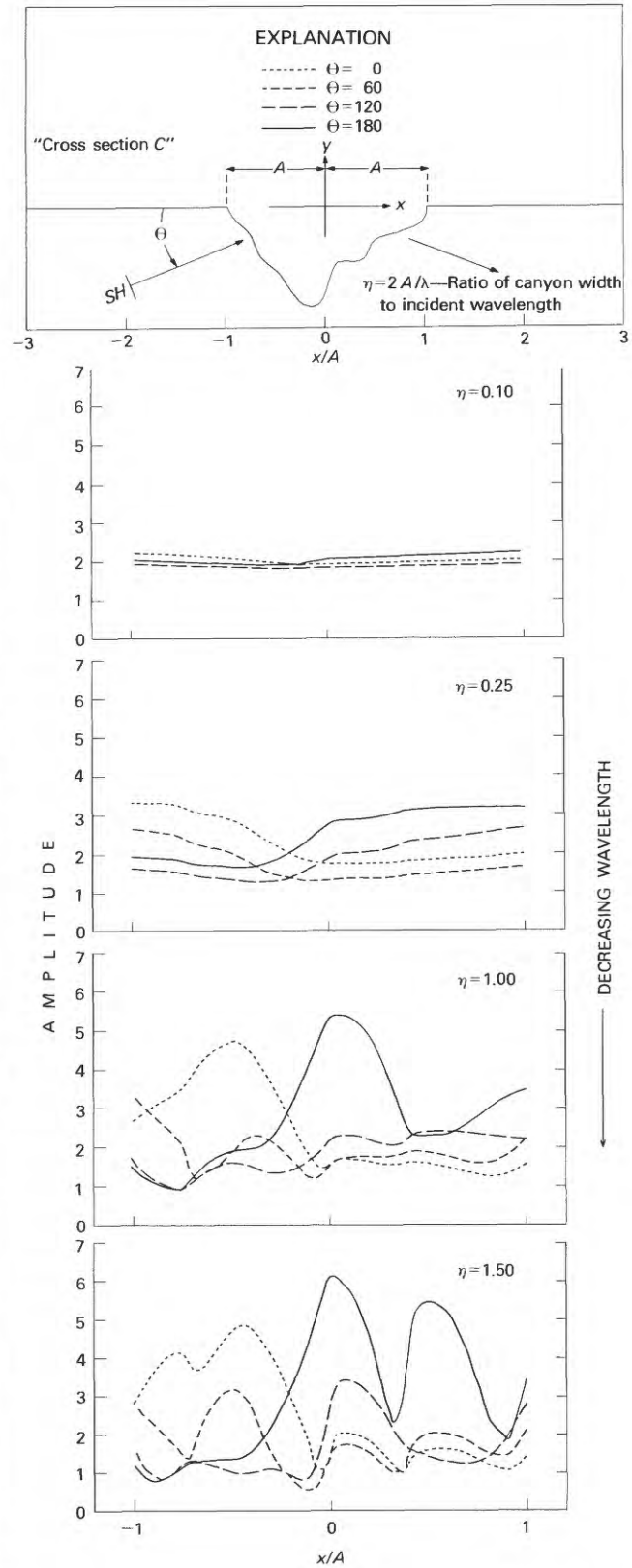


FIGURE 12.—Displacement amplitudes along surface of "cross section C" due to unit incident shear waves (SH) with angles of incidence θ of 0°, 60°, 120°, and 180° (after Wong and Jennings, 1975, fig. 3).

topographic amplification was an important factor affecting the landslide distribution in the Guatemala City area, as discussed below within the section entitled "Factors Affecting Landslide Concentration."

REGIONAL FRACTURE SYSTEMS

A well-defined system of regional lineaments exists in the highlands west of Guatemala City (fig. 13). This system, probably related to regional fractures, is noticeable on the U-2 photographs and the 1:50,000-scale topographic maps. The system is dominated by orthogonal elements trending N. 45° E. and N. 45° W. The origin of these lineaments is unclear; however, they have apparently provided a structural control on the major stream drainages in that area. This system of lineaments has also exerted an important, though indirect, control on the distribution of earthquake-induced landslides. These drainages have been filled with pumice during periods of volcanic activity and then reexcavated into canyons by erosion during periods of quiescence. The canyons now form optimal sites for rock falls and debris slides, as is evident from the landslide incidence in these canyons in response to the 1976 earthquake. One N. 45° E.-trending lineament near Tecpán and another near Chimaltenango, both of which showed a high level of aftershock activity, were interpreted by Langer, Whitcomb, and Aburto Q. (1976) to be secondary faults.

PREEARTHQUAKE LANDSLIDES

We also investigated the possible relation of preearthquake landslide deposits to the distribution of earthquake-induced landslides. Most such mappable features were large landslides or landslide complexes whose morphologies suggest deep-seated rotational slumps, block slides, or flows. Despite strong seismic shaking from the 1976 earthquake, preearthquake-landslide material mostly appeared to remain stable. Only at one site was a large part of an old landslide or landslide complex reactivated: cracks bounding the incipient landslide along the Río Cotzibal (fig. 14; site 9, table 1) were approximately along the margins of the preexisting landslide and extended throughout most of the preexisting landslide mass.

Earthquake-induced rock falls and debris slides were not uncommon within old landslide deposits, although these failures were typically restricted to steep toes and headwall scarps. For example, the landslide deposits near Laguneta del Tul, about 40 km northwest of Guatemala City (fig. 15), showed seismically induced rock falls along the steep headwall scarp and near the toe, where slopes had been steepened by stream erosion. However, no seismically induced cracks or other evidence of deformation were observed within the main

body of the landslide complex. A rancher who lives on this landslide complex reported that he could find no ground failures other than the above-mentioned rock falls despite a search he made of his land for earthquake damage.

Evidence from other earthquakes shows a similar behavior of dormant landslides during strong seismic shaking. Keefer, Wiczorek, Harp, and Tuel (1978) documented the fact that, in general, few dormant landslides are reactivated by earthquakes. Plafker, Ericksen, and Concha (1971) observed that most landslides in the 1970 Peru earthquake were rock falls and debris slides related to steep slopes rather than to preearthquake landslides. The behavior of old landslide deposits during the 1976 Guatemala earthquake implies that old landslides may be relatively stable even under conditions of strong shaking and indicates that the landslide margins near headwall scarps and eroded toes, where slopes are steepest, are the areas most susceptible to rock falls and debris slides.

LARGE INDIVIDUAL LANDSLIDES

Eleven large (greater than 100,000 m³ volume) landslides formed during the 1976 Guatemala earthquake; these landslides are described briefly in table 1. Here we describe in detail four of these landslides, of particular interest because they illustrate the various mechanisms by which large earthquake-induced landslides are formed and because they presented special hazards or potential hazards owing to blocked drainages and the subsequent floods created from breaching of the debris dams by impounded lake water. The three landslides at Los Chocoyos, San Martín Jilotepeque, and Estancia de la Virgen accounted for all the reported casualties in the highlands outside Guatemala City.

LOS CHOCOYOS

The Los Chocoyos landslide (figs. 16, 17; site 1, table 1) occurred about 15 km southwest of Tecpán, along the steep south wall of the valley of the Río Los Chocoyos. The slide buried two houses and killed six people. The slide mass contained between 0.75×10^6 and 1.0×10^6 m³ of debris, all derived from Pleistocene pumice deposits, primarily the tephra H and the H ash-flow tuff of Koch and McLean (1975). Witnesses to the landslide reported that they heard only one period of loud noise at the same time as the main earthquake shock. This report indicates that movement on the slide was rapid and that nearly all the slide material came down during the main shock.

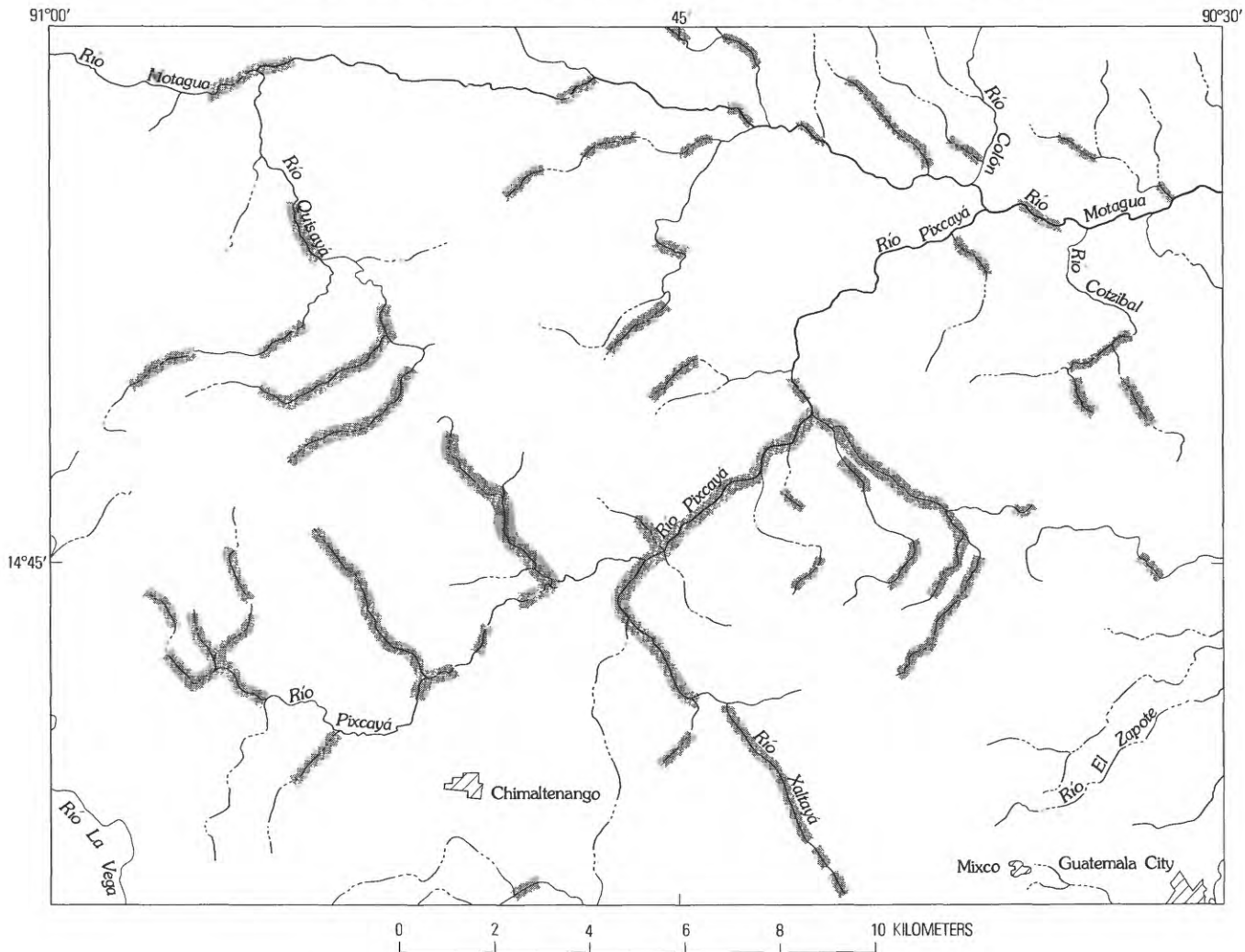


FIGURE 13.—Regional system of orthogonal lineaments (fractures?) in highlands west of Guatemala City. Shaded lines denote areas where lineaments apparently exert structural control on stream drainages.

Judging from the morphology of the headwall scarp and of the basal failure surface, the Los Chocoyos landslide probably began as a block slide and disintegrated into a debris avalanche that plummeted down the canyon wall to the river and then traveled some 600 m downstream before coming to rest. The slide debris filled the valley to a depth of 20 to 50 m over a length of about 800 m and a width of 300 to 400 m. The debris blocked the main river drainage and formed a lake that extended about 300 m upstream at its maximum (fig. 18). To avoid a sudden breaching of the debris dam and a consequent flood that could have endangered the villages and farms downstream along the Río Madre Vieja, volunteers from the Mexico Department of Transportation excavated a channel through the slide mass during the early stages of lake filling. The channel, however, did not initially accommodate a flow sufficient to drain the

lake, and as of May 1976 the lake was still rising. By late June the channel had widened (fig. 19) by erosion and sloughing of its banks, which finally allowed the lake to drain (fig. 20); and by the end of June 1976 the lake had drained completely.

The headwall scarp (fig. 21), between 50 and 60 m high, is formed by several intersecting fracture planes. Remnants of a planar basal shear surface are still present, dipping about 30° toward the river. The position and orientation of this shear surface indicate that it intersected the preearthquake valley slope about 20 m above the valley floor and that the landslide mass underwent initial free fall as it left the valley slope—a fact bearing on the mechanism of landslide emplacement, discussed below.

The face of one prominent fracture surface (fig. 21) trends approximately N. 70° – 80° W. and forms the right

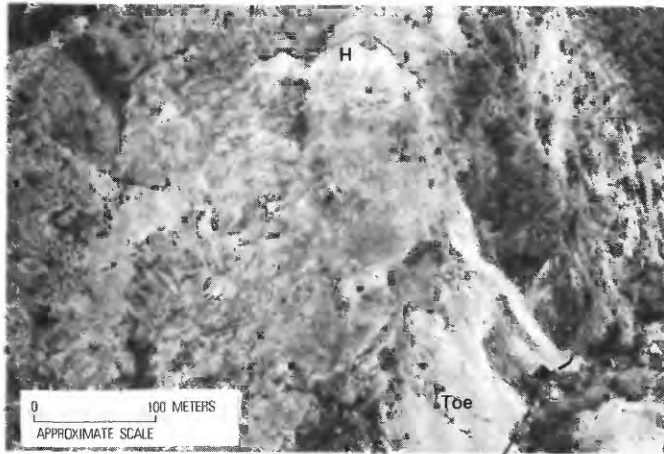


FIGURE 14.—Reactivated preearthquake landslide along Rio Cotzibal. Landslide mass is extensively fractured, but most movement consisted of debris slides from relatively steep toe (lower right, limit marked by dashed line). "H" marks headwall scarp.



FIGURE 15.—Old landslide complex at Laguneta del Tul, about 40 km northwest of Guatemala City. Rock falls occurred along headwall scarp (ridge on horizon) and at toe near stream (left foreground). Evidence of ground failure in main body of complex is absent. Note house (arrow) for scale.

(looking upslope, the southwest) flank of the headwall scarp; several other, less continuous fracture surfaces that trend approximately N. 20°–30° E. form the left flank. Weathering of parts of these fractures suggests that they are preearthquake surfaces which provided planes of weakness along which failure occurred. A slickensided lateral shear surface is on the downstream side of the failure scarp near the bottom of the valley slope (see figs. 16 and 17 for location).

The most prominent fracture cutting into the headwall scarp (arrows, fig. 21) extends as a ground

crack behind and above the right flank of the scarp. This fracture, which could be traced some 40 m to the southwest and had approximately 0.3 m of horizontal separation at the crown of the headwall scarp as of July 1976, outlines a large (about 100,000 m³ volume) wedge of bedrock partly dislodged by shaking. This incipient failure poses a definite hazard from future seismic activity to anyone reoccupying the Los Chocoyos village area.

Because the preearthquake center of mass of the Los Chocoyos landslide was approximately 100 m above the valley floor, the velocity of the landslide debris may have exceeded 100 km/h when the debris reached the valley bottom. After reaching the floor, the momentum of the debris carried it some 600 m downstream after it was deflected by at least 70° from the initial direction of downslope movement (see fig. 16). Despite horizontal translation and disaggregation of much of the landslide block, the original surface of the uppermost part of the block remained relatively intact. The original topsoil and much of the vegetation of the preearthquake slope remained on top throughout most of the areal extent of the slide; indeed, part of a cornfield even retained a semblance of rows after coming to rest.

A ridge of white pumice roughly 30 m wide and 10 m high forms the north boundary of the slide mass and extends along its entire north margin (fig. 22). The top of this ridge sits approximately 20 m higher than the adjacent mass of slide debris in the valley center. The granular pumice debris forming the ridge suggests that the debris is derived from the tephra H, approximately 2 m thick, that originally underlay the H ash-flow tuff, approximately 100 m thick, which constitutes the main slide mass. We propose this explanation because the pure-white ridge contrasts strikingly with the dark landslide debris, much as the white tephra H contrasts with the tan H ash-flow tuff (Hugh McLean, oral commun., 1976). Whitish pumice debris, which could be remnants of the tephra H, was observed along the basal failure surface.

Another interpretation of the pumice ridge is that the color contrast may be due to disaggregation and ejection of the pumice forming the ridge, because powdered or crushed rock commonly appears lighter in color than intact rock. Thus the pumice forming the ridge may be largely composed of the H ash-flow tuff instead of the tephra H.

The following observations suggest that the pumice ridge—whether of ash-flow tuff or tephra—was transported and deposited by the forceful ejection of disaggregated debris and air entrapped and compressed beneath the slide mass as it emerged from the slope and fell to the valley bottom. At the point indicated in the photograph (A, fig. 22), pieces of asphalt pavement as

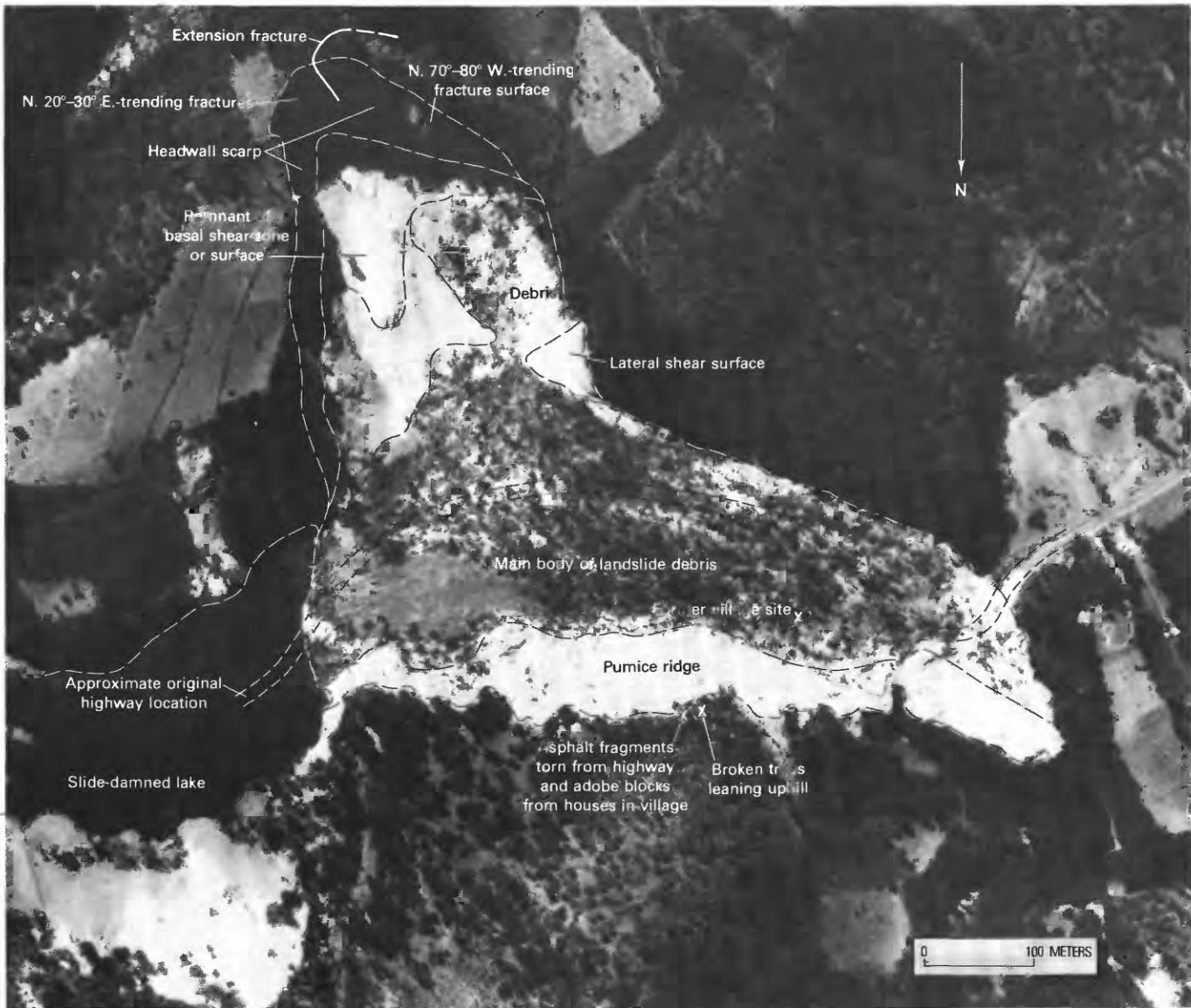


FIGURE 16.—U-2 photograph of Los Chocoyos landslide, showing main features outlined against countryside.

large as 2 m in diameter, apparently torn from the highway along the valley bottom near the river, along with several adobe bricks, presumably from houses of the village destroyed by the slide (V, fig. 22), were found immediately north of and upslope from the pumice ridge. Also, several trees just upslope from this ridge were broken near the bases of their trunks and were found leaning uphill away from the slide (T, fig. 22).

Although we were unable to determine the exact mechanisms governing the failure and subsequent movements of the Los Chocoyos landslide from an inspection of the field evidence, the basal failure surface and the steeply dipping extension fractures within the headwall scarp, as well as those forming the scarp itself, indicate

both shear and extension failure. Furthermore, the presence of an incipient failure outlined by the extension fractures in the headwall scarp suggests that these fractures formed before shear failure along the basal surface. Therefore, the probable sequence of events in the Los Chocoyos landslide was: (1) inertial forces from ground motion caused horizontal tensile stresses, leading to the formation of extension fractures; (2) these extension fractures propagated downward to an existing plane of weakness (the basal shear surface); (3) inertial forces within the slide mass were transferred to the basal surface as shear stresses; (4) the basal surface underwent shear failure, and the landslide was released; (5) all but the original surface of the landslide block largely dis-



FIGURE 17.—Los Chocoyos landslide, showing lake (left foreground) created by damming of Río Los Chocoyos. B, basal shear surface; D, landslide debris; H, headwall scarp; L, lateral shear surface.



FIGURE 18.—View eastward of lake dammed behind Los Chocoyos landslide, as it appeared in June 1976. Shattered pumice slopes are composed of tephra H and H ash-flow tuff of Koch and McLean (1975).

integrated either before or just after striking the bottom of the valley; the whitish granular pumice may have begun to be expelled at this time; (6) the landslide debris continued down the valley as an air-buoyed(?) avalanche; the white pumice ridge may have been emplaced during this phase; and finally (7) the landslide came to rest at its present position.



FIGURE 19.—View westward, downstream of channel (about 3 m deep) cut by stream from lake dammed by Los Chocoyos landslide; main body of landslide debris to right. Arrow indicates location of former highway pavement.



FIGURE 20.—View southeastward of lake dammed by Los Chocoyos landslide, showing level as of June 1976. Trees have been inundated by as much as 2 m of pumice debris derived from slides in river valley.

SAN JOSÉ POAQUIL

A landslide of about 3.5×10^6 -m³ volume occurred 2 km northeast of San José Poaquil (fig. 23; site 2, table 1). No occupied buildings were in the valley near the landslide, and no casualties were reported in the slide area. Witnesses living across the valley from the slide reported that it occurred during the main shock, and the sounds they heard indicated that the slide material moved rapidly. Other witnesses stated that noises from the landslide movement began several minutes after the main earthquake shock (E. Gobado, engineer, Centro de Estudios Mesoamericanos sobre Tecnología Apropriada (CEMAT), oral commun., 1978).

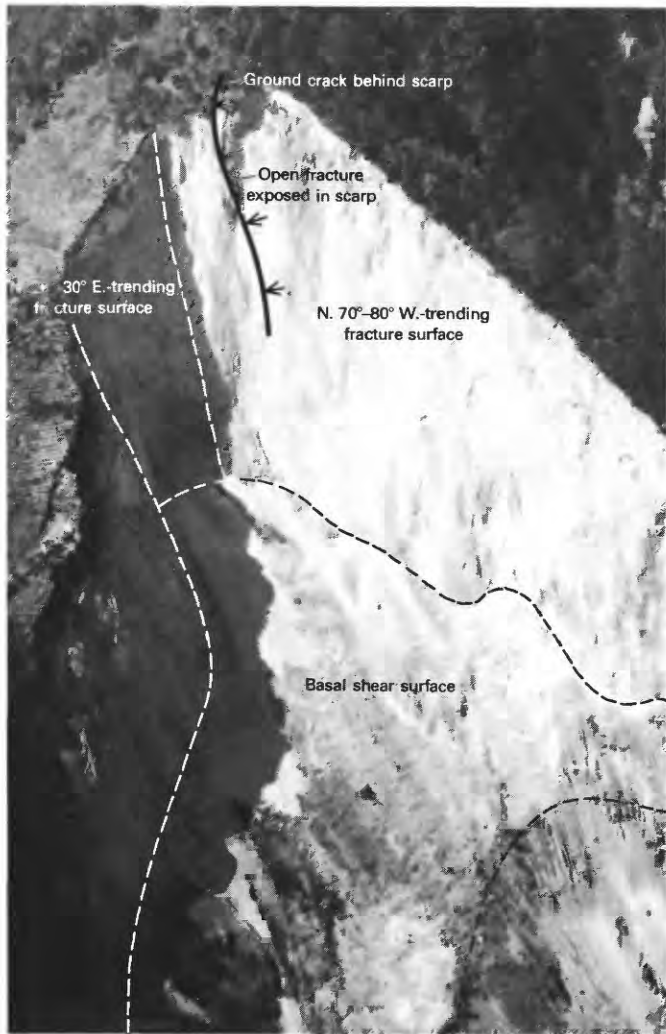


FIGURE 21.—View south-southeastward of headwall scarp (about 60 m high) of Los Chocoyos landslide. Note planar fracture surfaces forming scarp. See text for explanation.



FIGURE 22.—View northward of Los Chocoyos landslide, showing white pumice ridge along north margin; ridge debris is derived from material beneath main body of landslide (foreground). See text for explanation.

The landslide debris has a maximum thickness of about 50 m and extends approximately 1 km downstream from the foot of the headwall scarp. The landslide dammed the Rio Teculcheyá and created a lake about 1 km long and about 15 m in maximum depth. On June 27, 1976, the lake began to breach the landslide dam, though not catastrophically; and as of May 1978 the lake level was still slightly below that at which waters breached the landslide in June 1976.

The landslide formed as a complex rotational slump/avalanche in dark-gray to black welded tuff (WT, fig. 24) covered by a whitish pumice cap of irregular thickness (P, fig. 24). The age of the tuff is unknown. The pumice ranges from less than 1 to as much as 10 m in thickness (fig. 25). The welded-tuff fraction of the landslide debris (fig. 26) broke into blocky fragments, typically larger than 10 cm; the weakly cemented pumice disaggregated into sand-, gravel-, and cobble-size clastic fragments.

The headwall scarp (fig. 27) is about 35 m high and about 500 m long and strikes approximately N. 75° W. The planar surface of the scarp dips about 45° N. for 50 m downward from the top and then flattens to about 25° near the base (fig. 28). The scarp surface has two prominent sets of slickensides, the most prominent set plunging directly downdip and the other plunging northwest in the plane of the scarp, at about 30° to the first. A lateral scarp, intersecting the east end of the headwall scarp at nearly a right angle (fig. 29), is nearly vertical, trends N. 15° E., and extends along the slide margin for approximately 600 m (see fig. 23).

The landslide debris, about 50 m in maximum thickness, extends about 1 km northeastward from the foot of the headwall scarp. The landslide mass is a complex rotational slump/rock avalanche (see fig. 3) divided into three distinct zones (1-3, fig. 23). The material in zone 1 next to the headwall scarp (fig. 30) contains many secondary slumps spaced from 1 to 20 m apart. Most of this material remained relatively coherent despite at least 100 m of downscarp movement and about 20° of backward rotation. The original ground surface throughout most of this zone remained sufficiently intact during movement for the trees to continue to grow (as of July 1976), whereas trees in the slide debris further downslope in zone 2 (fig. 31) died. The slide material in zone 2 is much more internally deformed than the debris in zone 1; rock in zone 2 is extensively exposed on many secondary scarps. Still further downslope, the slide material in zone 3 exhibits flow features—for example, lateral ridges (shear surfaces along which landslide material has overridden adjacent intact material), longitudinal banding, and sinuosity conforming to the narrow valley walls. These features indicate that the debris in the toe (fig. 32) was sufficiently disaggregated to exhibit fluidlike flow.

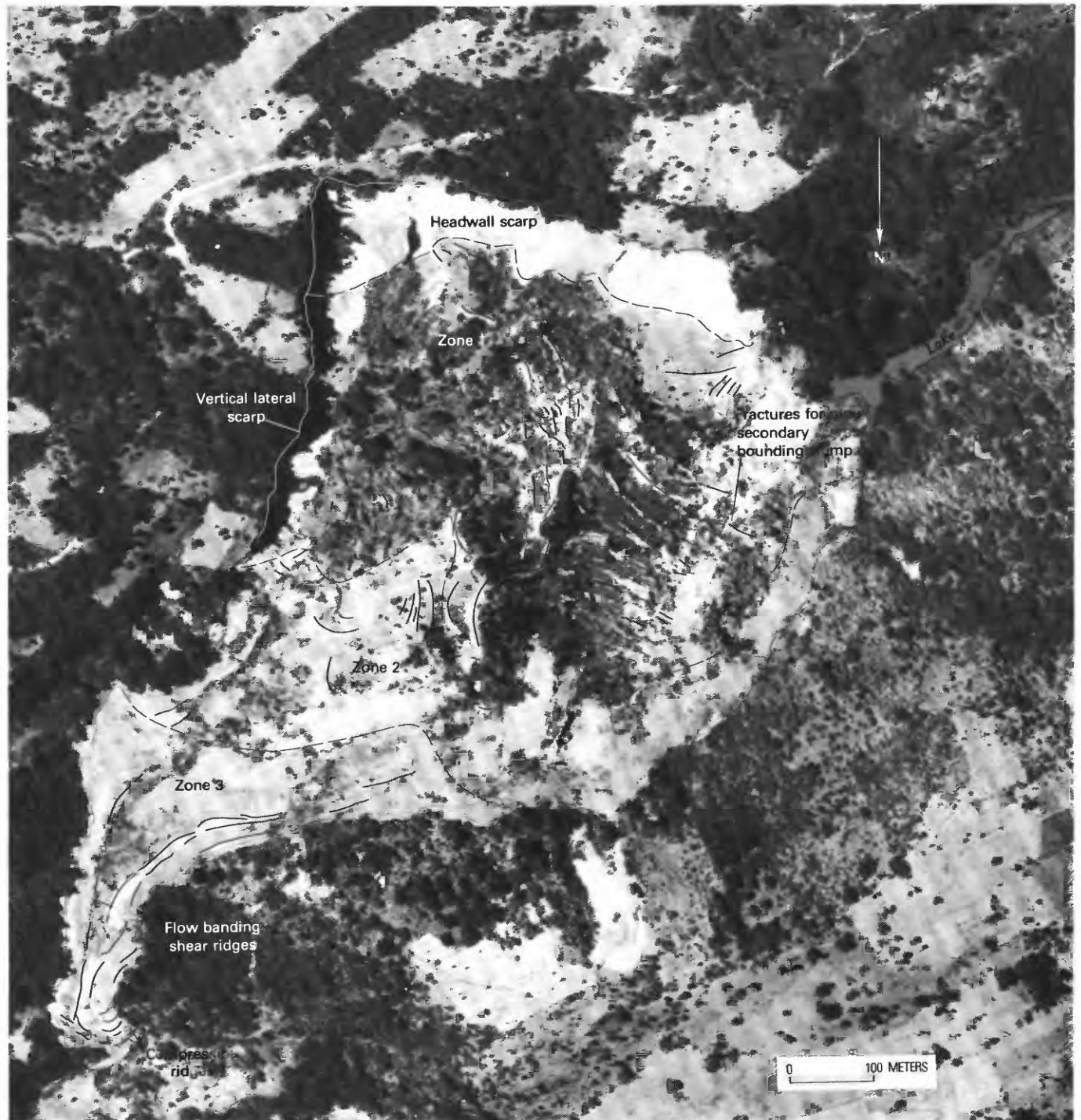


FIGURE 23.—U-2 photograph of large landslide 2 km northeast of San José Poaquil. Photograph taken February 13, 1976.

The location of the San José Poaquil landslide was influenced by two fractures that form the lateral and headwall scarps. The headwall scarp shows that shear failure occurred along a planar surface (the upper part of the headwall scarp) and that the failure surface curved

toward the horizontal beneath the landslide debris at the base of the scarp (see fig. 28). Curvature of the surface is also indicated by backward rotation of the slide-mass surface near the headwall scarp. Together, the nearly vertical fracture forming the east lateral scarp and the

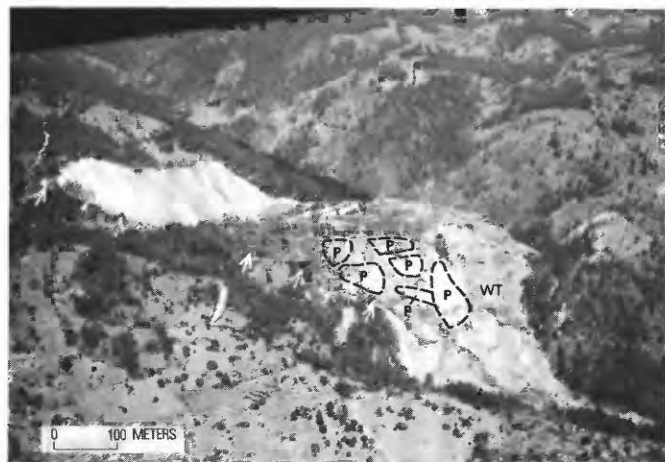


FIGURE 24.—San José Poaquil landslide; arrows denote lateral scarp. P, pumice; WT, welded tuff. See text for explanation.



FIGURE 25.—View northwestward of San José Poaquil landslide, showing contrast in color and texture between gray blocky welded tuff and white powdery pumice.

headwall scarp effectively confined the horizontal component of slide movement to the quadrant between N. 15° E. and N. 75° W. These fractures were also effective in limiting deformation because no fractures could be found above these scarps in the adjacent slopes. Assuming that all the striations on the headwall scarp were formed during the most recent landslide, slump movement of the rearmost slide mass was apparently in two distinct directions along the headwall scarp surface: one essentially downdip, and the other about 30° NW. on the same plane (fig. 27).

The fractures that form both the headwall and lateral scarps (fig. 28), which were traceable beyond the slide boundaries for several kilometers as lineaments, may be faults. The tarnished appearance of the lateral scarp in the photograph (fig. 28) is evidence that this surface is indeed a discontinuity which stood open as a fracture before the 1976 earthquake. Regardless of their previous

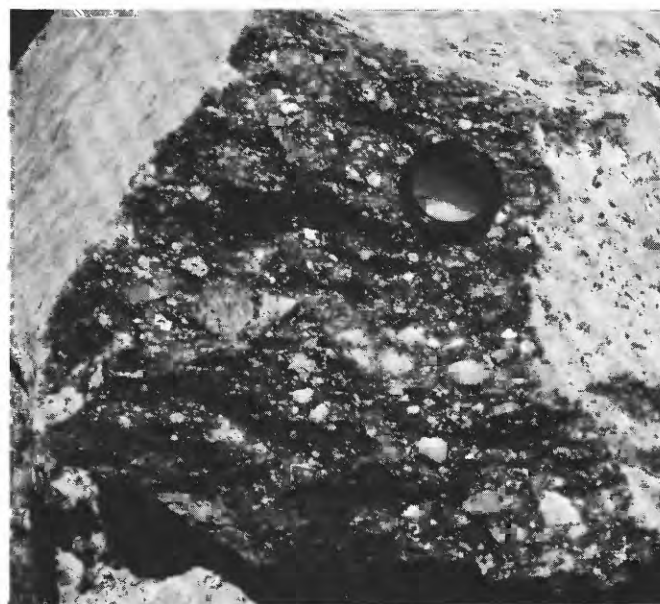


FIGURE 26.—Typical angular fragment of dark-gray welded tuff from San José Poaquil landslide.



FIGURE 27.—Headwall scarp of San José Poaquil landslide, showing two distinct sets of slickensides (dashed lines), one indicating dip slip, and the other oblique movement along plane of scarp.

history, the lateral and headwall scarps clearly served as planes of weakness that isolated the landslide mass dislodged by seismic shaking.

SAN MARTÍN JILOTEPEQUE

A landslide incorporating about 2×10^6 m³ of material occurred in pumice deposits approximately 2 km southwest of the village of San Martín Jilotepeque (figs. 33, 34; site 3, table 1). According to residents of the area, this slide destroyed 14 homes and killed 17 people. The landslide dammed the Río Quemayá and created a 250-m-long lake. Mexican highway workers trenched the



FIGURE 28.—Intersection of lateral scarp with headwall scarp of San José Poaquil landslide. Note freshly exposed rock (A), recently stained by rainfall washing, which contrasts with dark weathered surface of lateral scarp. Photograph taken in late June 1976.

landslide dam to drain the lake; the lake drained rapidly and caused a flood that swept away several villagers washing laundry about 3 km downstream (George Plafker, oral commun., 1976).

A witness who lived on a hillside across the river from the slide reported that he was awakened on the morning of February 4, 1976, by the earthquake. He described violent “stop-and-start movements” accompanied by loud rumbling and the sound of trees crashing together. The noises began during or shortly after the earthquake at 3:00 a.m. local mean time and continued periodically until 6:00 a.m. These periodic noises probably corresponded to episodic movements of the landslide.

The tongue-shaped north third of the landslide has a 20-m-high headwall scarp (H, fig. 34; fig. 35), the sinuous surface of which extends into intact pumice. Numerous extension fractures in the scarp area appear to be cracks extending from the headwall. Two distinct ridges (fig. 36) mark lateral shear surfaces across which landslide debris spilled as it rose above the adjacent ground. Similar, though much less distinct, features along the southeast lateral margin of this tongue have been largely obliterated by mixing of the slide material during its movement.

The northern tongue of the landslide mass slumped, moved horizontally at least 100 m across the valley, and dammed the Río Quemayá. Horizontal movement was estimated from measurements of the length of void space between the rear of the tongue and the headwall scarp, in the direction of slide movement. An examination of the headwall scarp, toe, and ridges of the northern tongue indicated that it ranges from 10 to 30 m in thickness and that the failure surface probably emerged from the slope near river level.

The southern part of the San Martín Jilotepeque landslide could be classified as a lateral spread because of the relatively gentle preearthquake slope of the slide mass and the extensive fissuring of the southern part (fig. 35). The area immediately to the north of this landslide is an older landslide, visible in 1961 aerial photographs, that morphologically resembles the northern tongue of the San Martín Jilotepeque landslide. No failures associated with this ancient slide were induced by the 1976 earthquake except at its headwall scarp (P, fig. 34), where some rock and soil falls occurred.

The south two-thirds of the earthquake-induced slide mass remains in an incipient state of failure. Within this mass, displacements of more than a few meters were restricted to steep slopes in the landslide toe near the river, where small debris slides extended downward to the river flood plain. This southern part of the landslide is pervaded by extensive fissures (fig. 35) that roughly parallel the main headwall scarp; other fissures were found as far as 50 m upslope beyond it. The largest differential vertical movements (as much as 3 m) were near the rear of the incipient mass, along a fracture extending from the headwall scarp of the northern tongue (arrow, fig. 35). As of July 1976, some additional movement may have taken place across some of these extension cracks as a result of renewed sliding caused by precipitation during the beginning of the rainy season; however, no positive field control was established to verify this observation. At that time, farmers were already moving back onto the landslide area to cultivate the landslide debris for the planting of crops.

In addition to the eyewitness account, several features of the landslide suggest that movement occurred in distinct pulses: at least two phases of movement are suggested by the presence of the two lateral shear ridges (fig. 36). The northern tongue of the landslide probably began as a series of retrogressive rotational slumps and proceeded downslope as an earth flow³ or series of block slides on a gently inclined (about 10°) failure surface, as indicated by the slope of the surface between the rear of the northern landslide tongue and the headwall scarp. The preearthquake topography had a surface slope of between 7° and 10° except in places adjacent to the river, where slopes were steeper than 40°.

Evidence of a water table above the basal slide surface suggests that this failure may have been caused by the liquefaction of granular pumice tephra. Agricultural wells in a cornfield just north of the northern tongue (fig. 36) showed a water level above the approximate height of the failure surface in that part of the landslide as of May 1976 (S. N. Hoose and R. C. Wilson, oral commun.,

³The term “earth flow” used here refers to a landslide characterized by tongue-like deposits on low slopes in which most deformation takes place by shear along the base and lateral margins, as described in detail by Keefer (1976) and Varnes (1978).

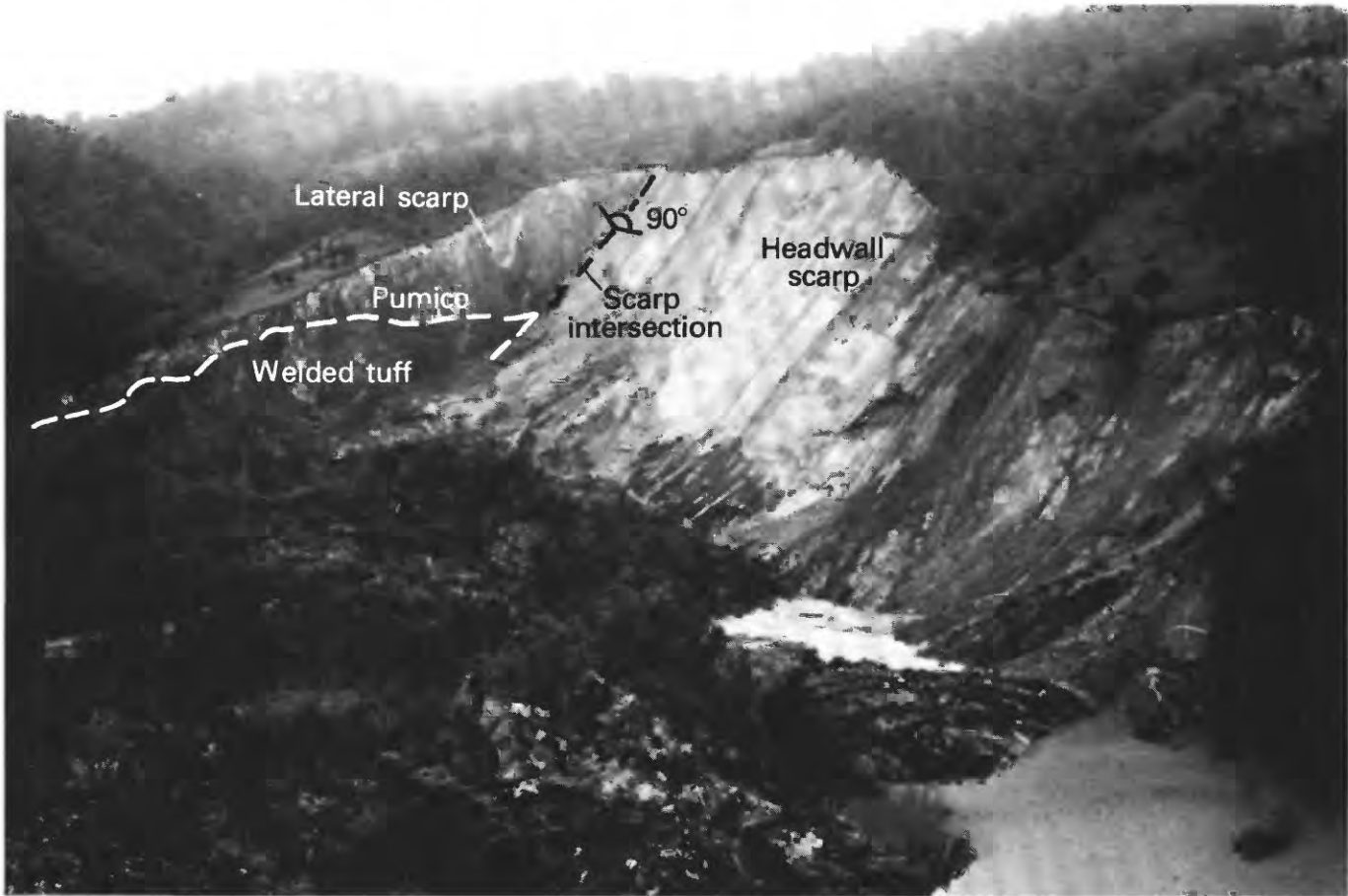


FIGURE 29.—View southeastward of San José Poaquil landslide, showing lateral and headwall scarps and contact between pumice and underlying welded tuff.



FIGURE 30.—View westward of part of San José Poaquil landslide mass near headwall scarp in zone 1 (fig. 23). Slide surface in foreground has remained coherent enough to preserve root structure of trees, which lean about 20°.



FIGURE 31.—View northward of material in zone 2 (fig. 23) of San José Poaquil landslide. Internal deformation of landslide mass has largely destroyed tree-root systems and killed trees, most of which had brown foliage as of late April 1976.



FIGURE 32.—View downslope in zone 3 (fig. 23) of toe of San José Poaquil landslide.

1976). Because no rain had fallen since the earthquake, the local water level was probably at least that high at the time of the earthquake, and so the pumice deposits at the landslide base may have been water saturated. In most places throughout the Guatemalan highlands, the air-fall tephra overlies paleosols that act as aquicludes. The porous overlying tephra is, therefore, a good reservoir of water (Hugh McLean, oral commun., 1976) and likely to liquefy under seismic shaking when saturated. Examination of the pumice deposits exposed in the headwall scarp of the landslide showed a sequence of ash-flow tuff units overlying a tephra unit that in turn overlies a paleosol. Because the pumice deposits are cyclic, with tephra units overlying paleosols, several other tephra units probably lie at depth.

During the earthquake, high pore-water pressures within the pumice deposits may have induced liquefaction and the slumping and lateral spreading that created the northern tongue of the landslide. This hypothesis requires that these pore-water pressures remained near overburden pressure without significant dissipation for at least the 3 hours during which sliding was observed to occur. Retrogressive slumping and shearing during downslope movement may have been sufficient to compact the basal slide material, elevate pore pressures, and maintain movement. No sand boils, dikes, or other direct evidence of liquefaction were found, however, except for lateral spreading of the landslide itself.

ESTANCIA DE LA VIRGEN

The large landslide near the village of Estancia de la Virgen (fig. 37; site 4, table 1) occurred in Tertiary

andesitic volcanic rocks capped by discontinuous pumice layers whose thickness ranges from a few meters to about 20 m. The landslide incorporated approximately 6×10^6 m³ of debris, part of which avalanched into the Río Pixcayá (fig. 38). The slide debris ranges in thickness from about 20 m near the toe of the avalanche to more than 50 m in places near the headwall scarp (H, fig. 38; fig. 39).

According to village residents, failure was sudden; slide debris crushed the houses built on the failed slope and killed their 13 inhabitants. The landslide dammed the river and impounded a lake that reached a length of 800 m before the dam was breached several days after the earthquake. Fortunately, the riverbanks downstream were uninhabited, and so the ensuing flood caused no additional casualties.

The morphology of this landslide suggests that it began as a series of rotational slump blocks (see fig. 3), parts of which disintegrated into blocky rubble that in turn formed an avalanche extending from the base of the headwall scarp to the river flood plain, where the debris extended across the Río Pixcayá to a depth of about 20 m. The rubble moved in discrete flow streams that developed flow banding and lateral shear surfaces within and along a well-defined troughlike avalanche chute (D, fig. 38).

The rotated slump blocks (A, B, figs. 37-39) indicate that the landslide began as a large rotational slump that was displaced about 100 m downslope. Much of the debris in the middle of the slide mass (D, fig. 8) continued moving and became an avalanche that flowed downslope to the river flood-plain terrace, crossed it as it spread laterally, and dammed the Río Pixcayá (fig. 40).

Blocks A and B of the landslide mass remained relatively intact despite a descent of more than 100 m. However, a tongue of debris (C, figs. 37, 38), which showed secondary slumping from the edges of block B, avalanched out onto the river flood plain and merged with the rest of the debris forming the landslide toe. The toe (figs. 37, 38) exhibited several distinct curvilinear lobes of debris that mark different flow fronts. These lobes may not indicate separate episodes of movement but rather changes in the flow direction of the debris during sliding.

Extension cracks (fig. 37, 39) were visible behind the headwall scarp for a distance of about 100 m (fig. 41). In late June 1976, slump movement was taking place along several of these fractures, probably as a result of precipitation during the rainy season. Several fracture-bounded blocks were reported to have slid down the scarp face in response to heavy afternoon rainfall. During this part of the rainy season, two ponds formed: one midway along the left margin of the landslide (looking upslope), and one near the base of the headwall scarp.

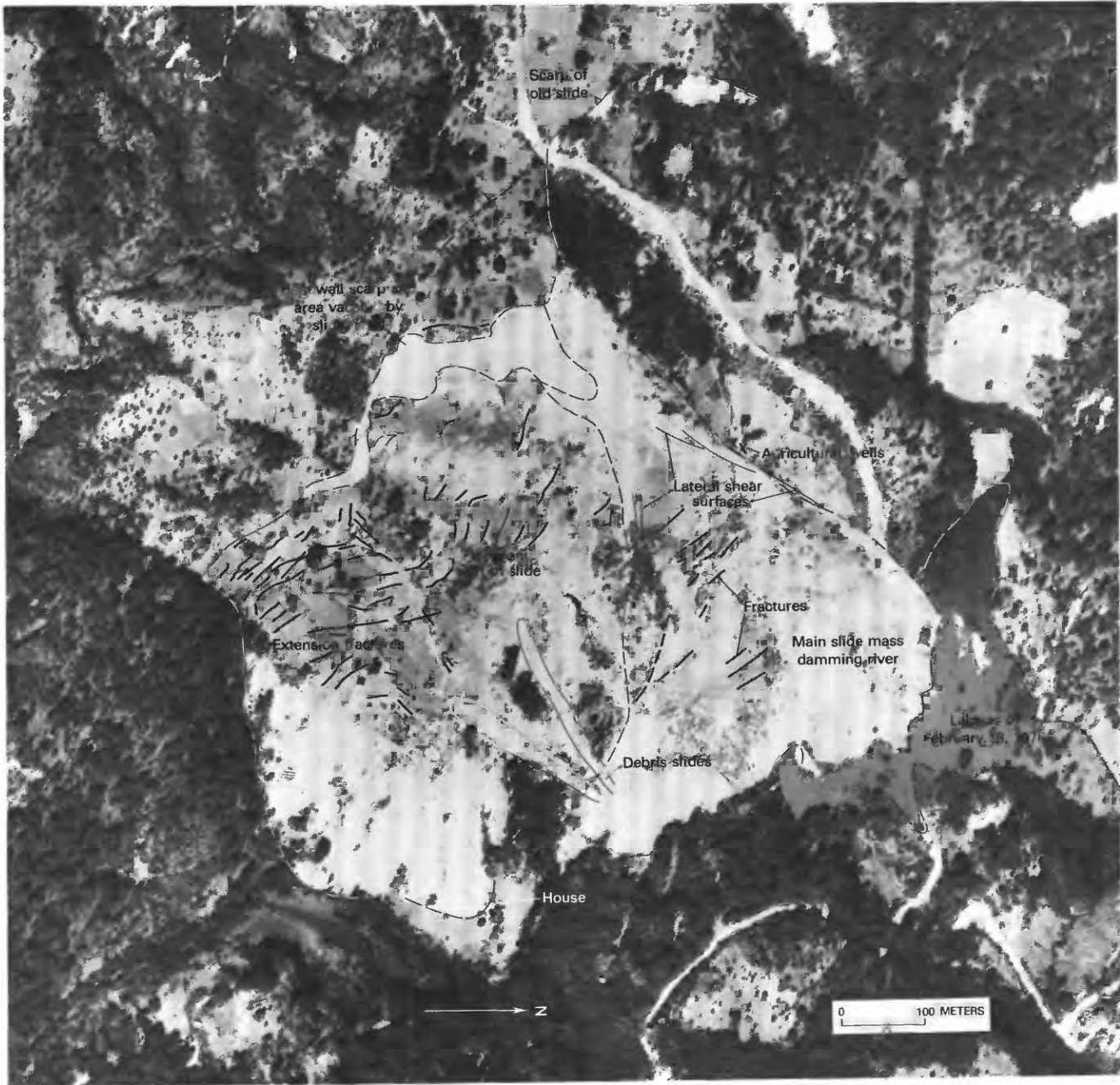


FIGURE 33.—U-2 photograph of large landslide 1 km southwest of San Martín Jilotepeque. Photograph taken February 13, 1976.

The Estancia de la Virgen landslide occurred in andesite deposits on a preearthquake slope of about 19° . The deposits were part of the toe of a much larger preexisting landslide complex that is about 3 km long parallel to the river and extends about 2 km normal to the river to its headwall scarp, which forms the ridge northwest of Estancia de la Virgen (see pl. 2). Throughout the older slide complex, seismically induced slope failures were confined to steep slopes on ridges and along the river. Although the landslide involved 6×10^6 m³ of material, it

involved only a small part of the older landslide complex. Otherwise, the main body of older landslide deposits was virtually unaffected except for several cracks that formed about 0.5 km northwest of the village. These cracks, the largest of which was about 50 m long, appeared to have formed within the topsoil as a result of ground shaking rather than from the formation of an incipient landslide. Village residents reported that no noticeable movement took place across these cracks even after the rains began.



FIGURE 34.—San Martín Jilotepeque landslide, a large lateral-spread/rotational-slump/earth-flow complex. Northern part, a tongue-shaped earth flow (dashed lines) that overran 14 dwellings, showed greatest displacement. Southern part is an incipient failure pervaded by numerous extension fractures (arrows). H, headwall scarp; P, headwall scarp of preearthquake landslide.



FIGURE 35.—Headwall scarp of San Martín Jilotepeque landslide, showing upper part of incipient failure and extension fractures pervading it. One fracture (arrow) is extension of scarp to right. Fractures in center and foreground indicate as much as 3 m of vertical movement.

OTHER LARGE LANDSLIDES

Of the seven other large landslides that blocked drainages (sites 5–11, table 1), all but two were rotational slumps in Tertiary volcanic rocks. Most of the

material in these slides disaggregated and moved sufficiently to produce rock avalanches from their toes. None of these avalanches had sufficient runout to travel more than several tens of meters, and most produced small lakes or ponds upstream from their debris dams. The Río Los Cubes landslide (fig. 42, site 11, table 1) south of Palencia appeared to be composed of Paleozoic(?) metamorphic rocks.

Several other landslides were not voluminous enough (20,000–100,000 m³) to dam stream drainages or otherwise to affect people or property. Three flow landslides occurred about 6 km north of Tecpán (pl. 1) in what appeared to be dark-brown soil overlying andesite. These landslides were observed only from the air, and the slide debris appeared to be wet soil that had flowed a great deal. The largest of these landslides is a long narrow feature (fig. 43) similar to the flows caused by liquefaction in the 1906 San Francisco, Calif., earthquake (Youd and Hoose, 1977). We have no data on the moisture content of this landslide, however, and therefore no evidence of whether liquefaction occurred there.

Another long narrow landslide (fig. 44) of about 100,000-m³ volume occurred in dry pumice deposits near Finca San Carlos, about 16 km northeast of Guatemala City. The slide began as a rotational slump and became an avalanche that traveled about 300 m downslope.

A large incipient failure occurred near El Zarzal, about 22 km north of Guatemala City, where ground cracks clearly outline a rotational slump of about 300,000-m³ volume displaying 1.2 m of displacement along the headwall scarp. The headwall scarp of this slump (fig. 45) is about 20 m northwest of a N. 55° E.-trending fracture or fault that forms a regional lineament noticeable on aerial photographs and also on the 1:50,000-scale topographic maps. The rotational slump, which occurred in Tertiary andesitic rocks and other volcanic material, is a reactivated part of an ancient landslide. Revisiting the site 2 years after the earthquake, we could measure no further movement along the headwall scarp despite the effects of two rainy seasons.

Although most of the large landslides (table 1) occurred on relatively steep slopes, we noted few common factors influencing their distribution. The occurrence of seven of these landslides in the Tertiary andesitic volcanic rocks does not, in itself, mean that these rocks were the most susceptible to large landslides, because they account for 70 percent or more of outcrops in the western highlands. Because of the apparent absence of common controlling factors, we know of no way to predict the locations of large seismically generated landslides in Guatemala on a regional basis.



FIGURE 36.—View southwestward of inner (IR) and outer (OR) lateral shear ridges on north margin of northern tongue of San Martín Jilotepeque landslide. Inner ridge was formed during later surge of movement than outer ridge. X, agricultural well.

LANDSLIDE CONCENTRATION IN THE GUATEMALA CITY AREA

Because landslides in such a heavily populated area as Guatemala City have a severe impact on people and property, the pattern of landslide occurrence from the 1976 earthquake is extremely important in providing information concerning the probable distribution of similar landslides in future earthquakes. For this reason, we studied the earthquake-induced landslide distribution in the Guatemala City area in detail to determine whether the distribution was influenced mainly by site conditions or by factors unique to this particular earthquake.

Our map (fig. 46), which depicts the relative abundance or concentration of landslides generated in the Guatemala City area by the 1976 earthquake, is a generalization of an unpublished 1:12,500-scale landslide inventory prepared from aerial photography and field reconnaissance. Thus, this landslide concentration map is a second-generation map that quantifies and categorizes the concentration of landslides along discrete areas of the canyon margins to which earthquake-

induced landslides were confined. We believe that this map usefully illustrates the landslide distribution for the purposes of planning and decisionmaking in Guatemala City.

We calculated landslide concentrations in the following manner (fig. 47). The concentrations (percentage of slope length failed) of landslides in discrete 0.5-km-long segments of canyon were determined by measuring the widths of landslide scarps along a given segment, totaling these widths, and dividing by the total length of a given segment (0.5 km). Because virtually all landslides in the Guatemala City area were thin rock falls or debris slides, and because most housing developments near the canyon margins are on the plateau above the upper rim, a landslide concentration based on the scarp width was considered to be a better measure of canyon-wall stability than one based on the scarp area or area of landslide debris covering the canyon bottom. Landslide concentrations were then categorized as low (0–5 percent), moderate (5–20 percent), high (20–50 percent), or severe (greater than 50 percent).

We consider the calculated landslide concentrations to characterize the susceptibility or extent of failure of dif-

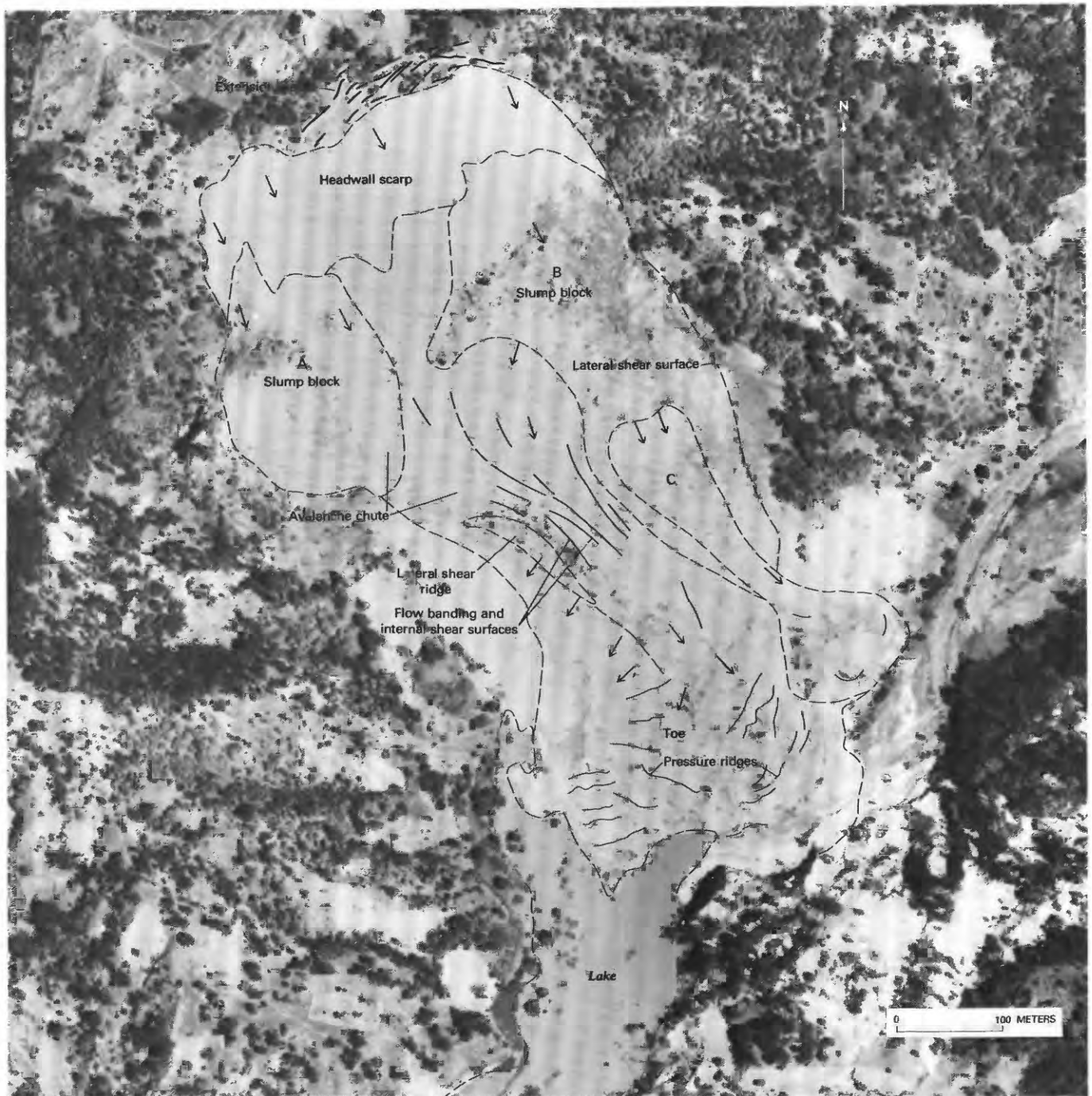


FIGURE 37.—U-2 photograph of large landslide near Estancia de la Virgen. Photograph taken February 13, 1976. Arrows show direction of slide movement.

ferent canyon-wall segments. These concentrations are displayed as zones that extend from the uppermost extent of the landslide scarps to the canyon bottoms along the 0.5-km-long segments. Most canyons are so narrow

that respective landslide concentration zones of opposite canyon walls meet at the bottom. A few canyons southwest of Guatemala City have extensive flood plains along the canyon floors, where landslide debris covered

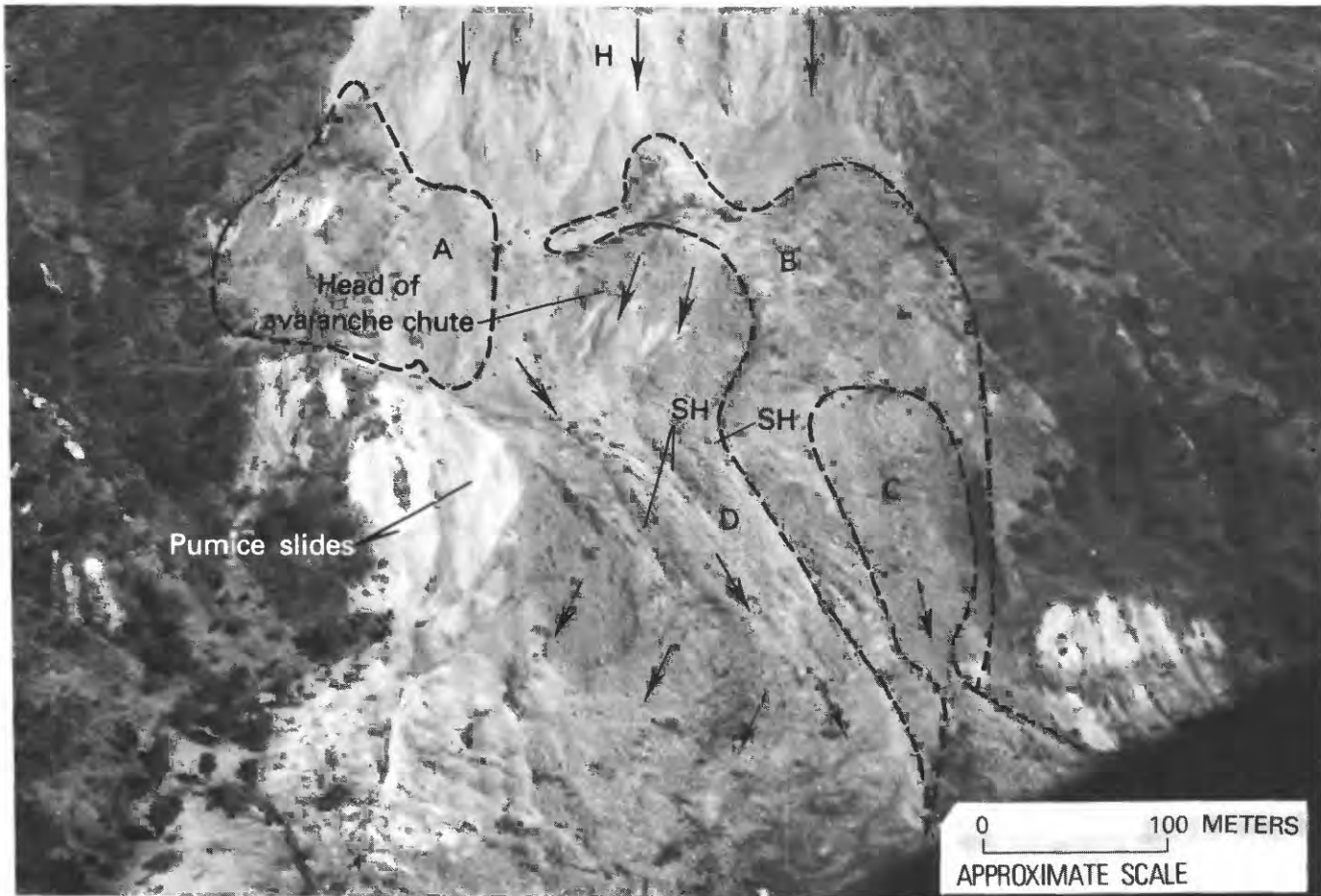


FIGURE 38.—View north-northeastward of Estancia de la Virgen landslide; arrows indicate direction of movement of avalanche debris. A and B, rotated slump blocks; C, head of secondary rotational-slump avalanche within slump block B; D, center of avalanche chute; H, headwall scarp; SH, shear surfaces.

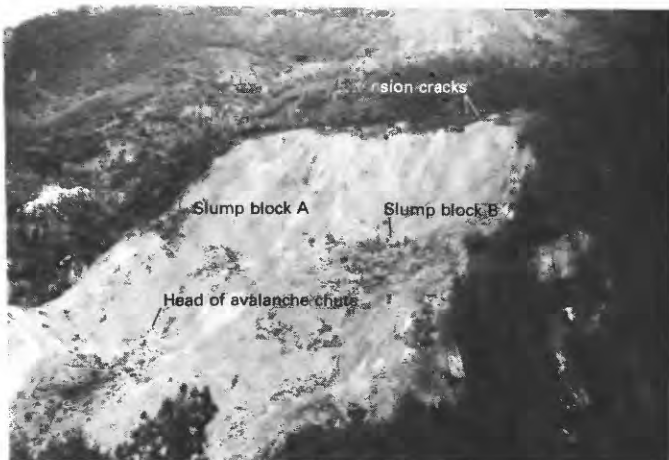


FIGURE 39.—Oblique aerial view of headwall scarp and associated features of Estancia de la Virgen landslide.

parts of the relatively flat terrain adjacent to the canyon walls. There, the landslide concentration zones include not only the canyon walls but also parts of the flood plains.

As can be seen on our landslide concentration map (fig. 46), canyon slopes were not uniformly affected by seismically induced landslides. For example, in the central part of the map area along the Río La Barranca, landslide concentration zones classified as moderate and severe are juxtaposed. Immediately to the north, severe concentrations are adjacent to low and moderate concentrations along the Río El Naranjo. The canyon slopes of the Río El Naranjo were markedly unaffected by landslides, although the slopes are in an area practically surrounded by canyons with high and severe landslide concentrations. Landslide concentration also varies greatly in the area north of Guatemala City as well as

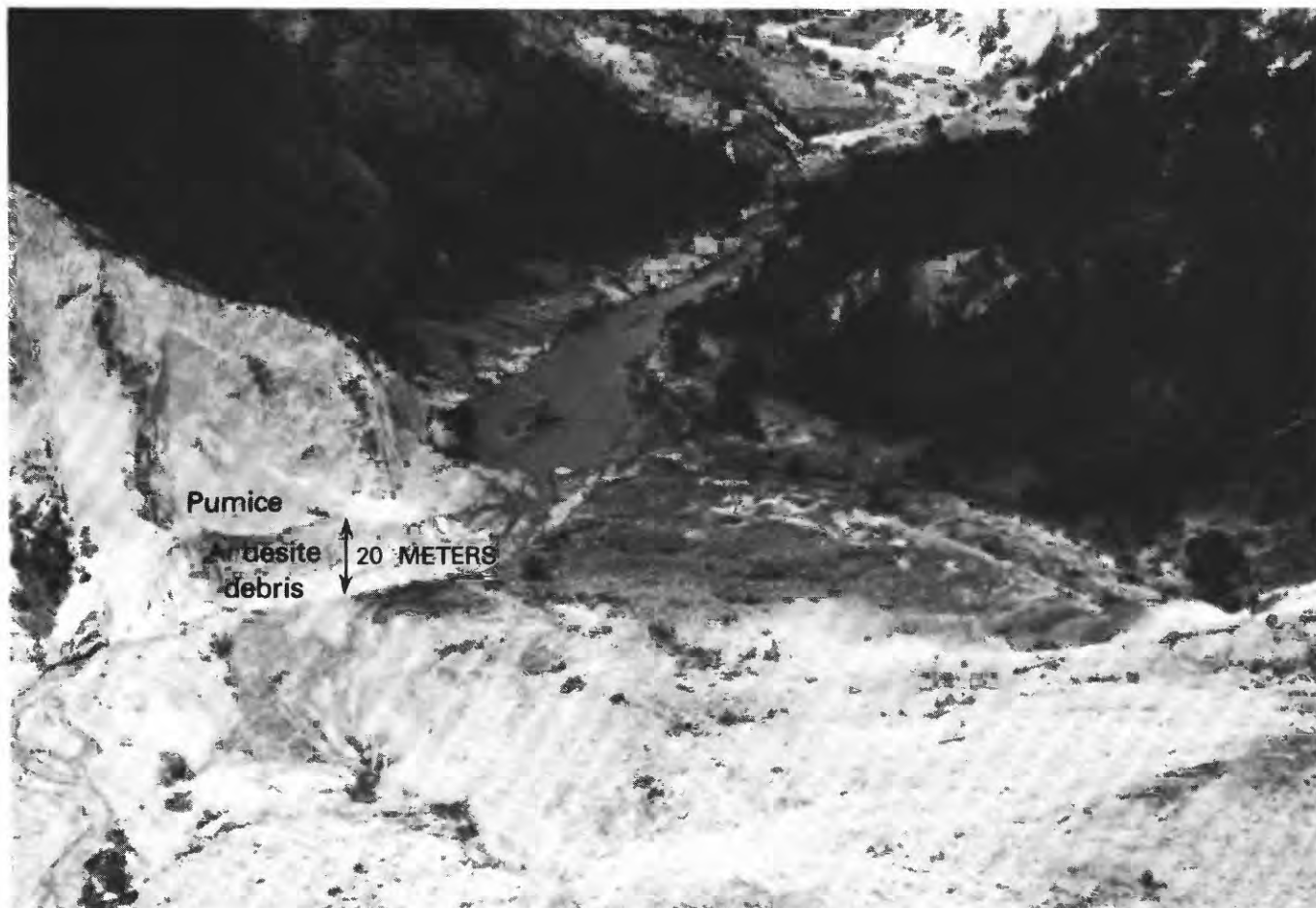


FIGURE 40.—Toe of Estancia de la Virgen landslide, showing andesitic debris damming Río Pixcayá. Remains of debris dam are visible (left center) where stream has cut a channel through debris. Note contrast between dark andesite and light-colored pumice debris.

along many of the canyon slopes to the southwest. These examples indicate extreme differences in landslide susceptibility in many places along the canyon slopes.

FACTORS AFFECTING LANDSLIDE CONCENTRATION

An analysis of the landslide concentration patterns suggests that the landslide incidence from the 1976 earthquake within the network of canyons in the Guatemala City area has been influenced by the following geologic and seismologic factors, in addition to steep canyon slopes: (1) lithology, both of bedrock and of the overlying residual soil; (2) preexisting fractures; and (3) severity of seismic shaking as amplified by slope geometry.

LITHOLOGY

Although virtually the entire Guatemala City area is underlain by Pleistocene pumice deposits, the landslide

concentration appears to have been influenced by lateral variations among the rocks and residual soil of these deposits. Exposures in vertical canyon walls in the Guatemala City area show that individual units within the pumice deposits vary greatly in thickness within horizontal distances of only tens of meters (fig. 48).

Although all the pumice deposits have extremely low tensile strength, differences in sorting and grain shape also influence the strength of deposits. The tephra, for example—the product of airborne ash falls—are less dense, better sorted, and hence generally more friable (that is, of lower tensile strength) than the ash-flow tuffs. The tuff units are generally poorly sorted, un-reworked, nearly unstratified mixtures of coarse ash, pumice, and lithic fragments. The tephra units are generally only several meters in maximum thickness in the Guatemala City basin, whereas ash-flow tuff constitutes the bulk of the basin fill (Koch and McLean, 1975). Because of lateral variability in the thickness of the pumice units, the relative percentages of the dif-

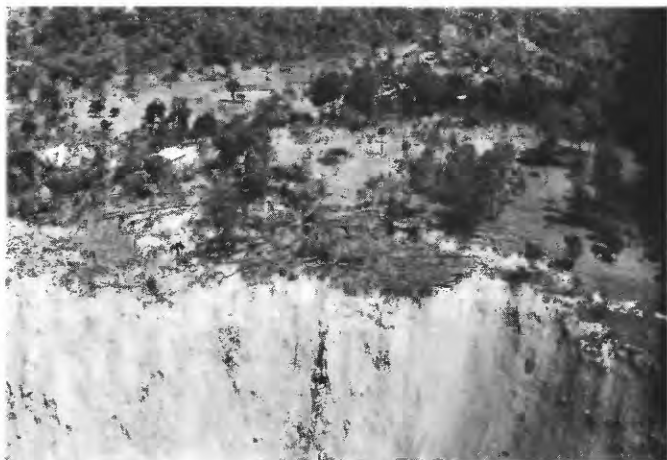


FIGURE 41.—Extension cracks above headwall scarp of Estancia de la Virgen landslide.



FIGURE 42.—View northward of Río Los Cubes landslide south of Palencia.

ferent pumice deposits within a vertical sequence may vary greatly over short distances. Such variations result in differences in rock strength and are probably responsible for much of the variability in rock-fall concentrations within the canyons.

A striking example of lithologic control on landslide concentration is the lithologic variations in the pumice deposits and overlying residual soils and the effect of these variations on the relative abundance of different landslide types. Within the Guatemala City area, debris slides were scarce in comparison to rock falls, whereas along the Río Motagua, 25 km north of Guatemala City, debris slides were far more abundant. In Guatemala City the soil on pumice deposits is typically 1 to 2 m thick, consists mainly of sand-size pumice particles, and contains small amounts of clay that provide sufficient cohe-



FIGURE 43.—U-2 photograph of flow landslide north of Tecpán.

sion to inhibit the formation of debris slides. The pumice soil along the Río Motagua is thinner (less than 0.3 m thick) and contains little organic material or clay. This northward decrease in soil thickness and clay content coincides with a rain shadow to the north of the Continental Divide, which transects Guatemala City. The arid conditions to the north along the Río Motagua may inhibit the formation of clay and organic material in pumice soil there.

The pumice deposits are also thicker, more massive, and support steeper slopes (Hugh McLean, oral commun., 1978) in the Guatemala City area than to the north. Along the Río Motagua the pumice deposits are mainly fluviolacustrine, whereas the pumiceous strata in the Guatemala City area are composed of massive ash-flow tuff units interbedded with tephra and minor fluviolacustrine deposits. The pumice deposits in the Guatemala City area have a maximum thickness of over 100 m, whereas those along the Río Motagua are no thicker than 30 m (Hugh McLean, oral commun., 1978). Slopes composed mainly of subrounded fluvial pumice gravel and lacustrine deposits along the Río Motagua are



FIGURE 44.—Rotational slump/avalanche in pumice deposits near Finca San Carlos. Length of landslide from headwall scarp to toe is estimated to be 200 m.

not so steep as those in the Guatemala City area, which are composed primarily of ash-flow tuff and tephra whose primary particles are highly angular and interlock to provide sufficient cohesion to support nearly vertical slopes. As a result, the ash-flow tuff and tephra in the Guatemala City area and their overlying soil failed as rockfalls, whereas the pumice deposits along the Río Motagua produced mainly debris slides. Therefore, a combination of factors—lithology, soil thickness, slope steepness, and soil clay content—appear to account for the north-to-south gradational decrease in the ratio of debris slides to rock falls.

FRACTURES

The spacing and orientation of preexisting fractures may also have influenced the concentration of seismically induced landslides in the Guatemala City area. In many places, we interpret the nearly vertical



FIGURE 45.—Incipient rotational-slump landslide near village of El Zarzal. Arrows mark headwall scarp.

weathered planar surfaces forming part of the scarps of rockfalls to be preexisting fractures that served as planes of weakness. We observed that other vertical weathered fracture surfaces intersect the scarp surfaces. In the Guatemala City area, a strongly preferred orientation of N. 10°–20° E. was observed in fractures exposed in the rock-fall scarps; this orientation approximately parallels the Mixco fault zone.

TOPOGRAPHIC AMPLIFICATION

Because seismic shaking served to trigger these landslides, we expected the landslide concentrations to correlate with isoseismals from the 1976 earthquake. On a regional scale (see fig. 2), they do seem to correlate because the highest landslide concentrations fall within the highest intensity isoseismals. At a larger scale, however, a correlation between isoseismals and landslide concentrations is no longer apparent (fig. 49). Within the Guatemala City area the landslide concentrations are inconsistent with the intensity data; both high and low landslide concentrations are found within areas of MMI VI, VII, and VIII contours, and the landslide concentrations show no apparent conformity with the isoseismals. Nonetheless, a noticeable relation of landslide concentration to slope geometry suggests that the level of ground shaking (or seismic intensity) within the canyons varied greatly over distances of about tens of meters.

Topography appears to have influenced the concentration of landslides within the canyon network of Guatemala City in a manner similar to that discussed

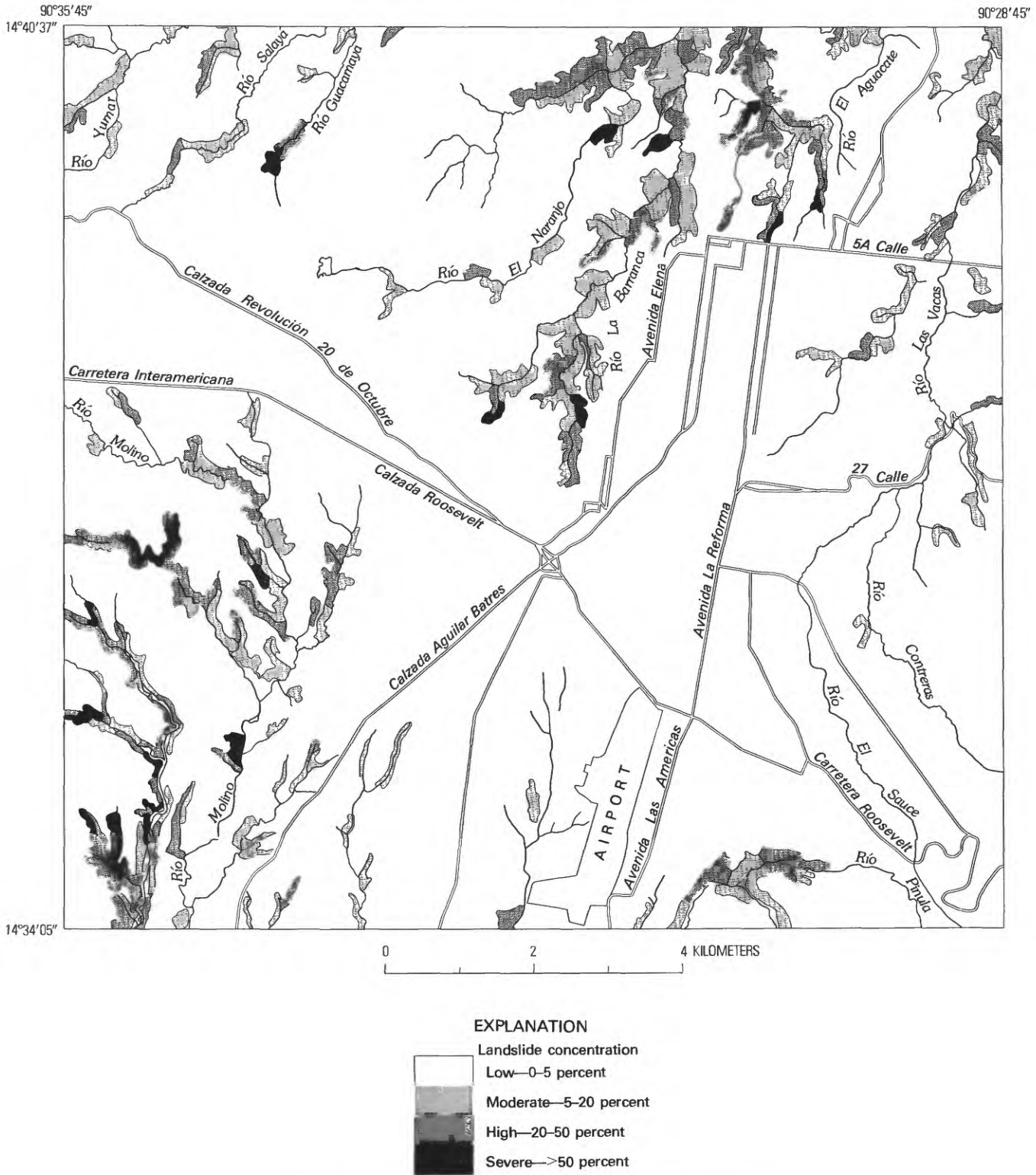


FIGURE 46.—Landslide concentration map of Guatemala City area.

above in the subsection entitled “Amplification of Ground Motion by Topography.” In the Guatemala City area, topographic amplification appears to have sub-

stantially increased the shaking intensity over distances as small as tens of meters. In many places, ridges and promontories exhibited high concentrations of rock falls,

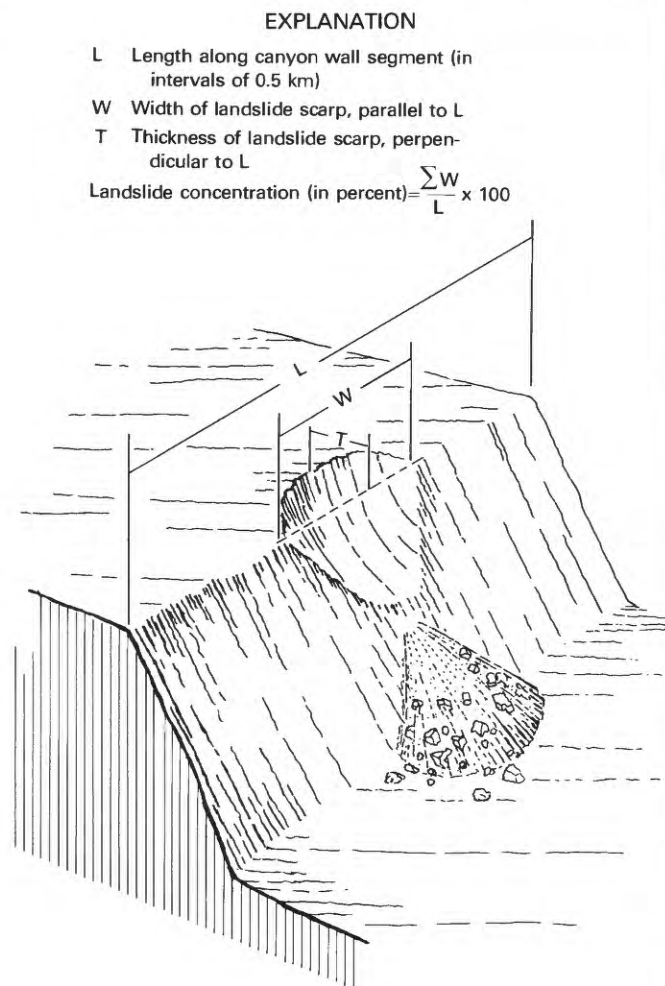


FIGURE 47.—Diagram illustrating method of calculating landslide concentrations for map in figure 46.

whereas nearby slopes remained relatively unaffected (fig. 50). Observations of this topographic effect were largely confined to unpopulated canyon slopes. Consequently, this effect is not evident in the intensity data gathered by questionnaire by Espinosa, Husid, and Quesada (1976).

The inconsistency between the observed landslide distribution and isoseismals for the Guatemala City area points out the significant difference between an intensity survey and a ground-failure survey, because the two surveys commonly sample both different territory and different phenomena. The intensity survey reflects bedrock ground shaking, site conditions, and structural behavior, whereas the ground-failure survey reflects bedrock shaking and the numerous complicated factors that influence the site conditions of steep slopes, commonly in unpopulated areas not covered by intensity surveys. In Guatemala City these two basic types of information, not commonly gathered together, complement each

other and point up a few of the inconsistencies (Espinosa and others, 1978) that can arise in the absence of a thorough examination of both ground-failure and shaking-intensity distributions. Taken together, the two types of survey can, however, provide a clearer understanding of both landslide distribution and variations in ground motion.

The majority of our field observations suggest that lithology and topography were the two most influential factors affecting the landslide concentration in the Guatemala City area. This evidence for the influence of physical site conditions on landslide distribution is of great importance in answering the question whether future earthquakes will produce similar landslide concentrations, given different earthquake-source parameters.

RECOMMENDATIONS FOR REDUCTION OF SEISMICALLY INDUCED LANDSLIDE HAZARD IN GUATEMALA CITY

Despite the high landslide incidence from the 1976 earthquake, the overall physical characteristics of canyon slopes in the Guatemala City area remain essentially unchanged today. Areas of high and severe landslide concentrations from this earthquake also are likely to be sites of landslide activity in future earthquakes. Future earthquakes with much stronger ground shaking, longer duration, and markedly different source characteristics, however, may cause additional failures on slopes other than those that failed in 1976. Steep canyon slopes cannot be assumed to be safe simply because they did not fail in the 1976 earthquake. Rather, we consider all areas of high and severe landslide concentrations in the 1976 earthquake to be those most susceptible to future seismically induced landsliding.

Because few seismically induced landslides in the Guatemala City area were thicker than 10 m, approximately 95 percent of the landslide areas could have been avoided if dwellings and other buildings had not been closer than 10 m to the canyon margins or had not been built along the canyon slopes below the plateau rim. Therefore, future placement of such critical structures as hospitals, communication systems, schools, and dwellings should avoid all areas within or near the canyon margins that were in zones of high or severe landslide concentration in the 1976 earthquake.

SUMMARY

The total of more than 10,000 landslides triggered by the 1976 Guatemala earthquake makes this earthquake one of the most significant in recent history in terms of generating ground failures. Because of the widespread



FIGURE 48.—Headwall of Rio Guacamaya barranco, showing great lateral variation in thickness of pumice deposits; note jeep in upper left corner for scale. Labeling of units is according to Koch and McLean (1975, fig. 11). Photograph courtesy of Hugh McLean.

landslide distribution, the 1976 earthquake has provided a great deal of information and insight regarding seismically induced landslides, particularly rock falls and shallow debris slides. Our photointerpretation, photomapping, field reconnaissance, and statistical investigation of these landslides lead us to the following generalizations.

(1) The predominant types of landslides generated by this earthquake were shallow rock falls and debris slides. Rock falls most commonly occurred on slopes steeper than 50° , were generally thinner than 6 m, and appeared to be tensile failures resulting from the reflection of seismic waves off canyon walls. Debris slides occurred on

gentler (30° – 50°) slopes within thin noncohesive soil layers on Pleistocene pumice deposits.

(2) The regional distribution of landslides resembles the overall pattern of seismic intensities. The threshold intensity for triggering small rock falls and debris slides was an MMI of approximately VI.

(3) Although Pleistocene pumice deposits occupy only about 20 percent of the earthquake-affected region, 90 percent of the seismically induced landslides occurred in these deposits. Most other landslides occurred in Tertiary andesitic volcanic rocks, which are widespread.

(4) Virtually all landslides were on steep slopes and within canyon topography. The concentration of land-

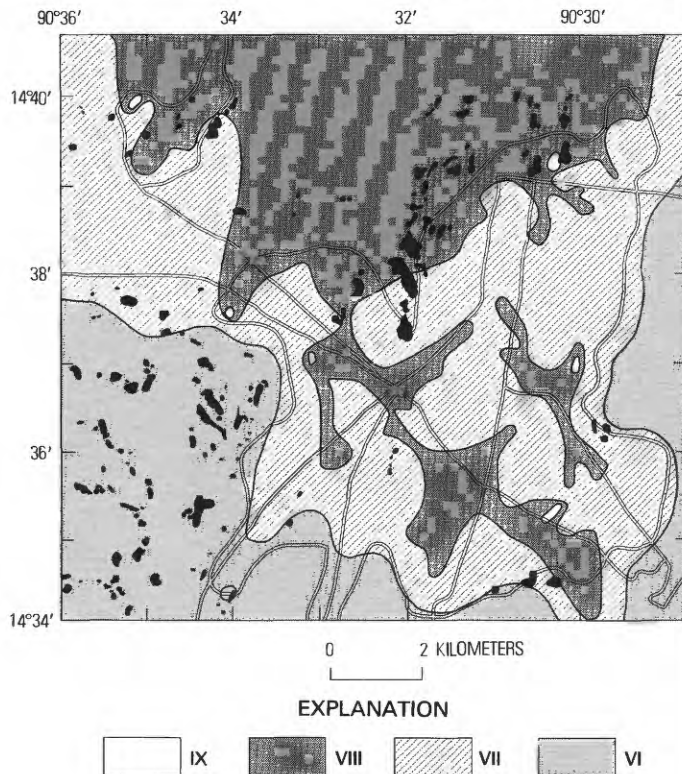


FIGURE 49.—Distribution of seismic intensities and landslides (black areas) from 1976 Guatemala earthquake in Guatemala City area. Note scatter of landslides throughout areas within zones of MMI VI, through VII (after Espinosa and others, 1978, fig. 25).

slides in these areas was apparently due to the combined effects of the steepness of canyon walls and the amplification of seismic ground motion by canyon geometry.

(5) The presence of regional fractures, which directly influenced the regional landslide distribution, provides zones in which thick pumice deposits have accumulated. The steep-walled canyons subsequently eroded through the pumice are particularly susceptible to failure during earthquake ground shaking.

(6) The presence of preearthquake landslides did not contribute to slope instability during this earthquake. The obvious preearthquake landslides, mainly deep-seated rotational slumps, block slides, or flows, showed little reactivation during the 1976 earthquake.

(7) The 11 large landslides presented a hazard to people and property not only from mass movement but also from subsequent damming of streams, flooding, and breaching of the landslide debris by lake waters. Fortunately, because all of the affected areas were sparsely populated, the damage done in this way was relatively small. Although most of these large landslides were associated with relatively steep slopes, we could discern no common factors influencing their distribution, owing to small size of the sample group.



FIGURE 50.—Housing development in northeastern Guatemala City, showing extensive rock falls and bedrock fractures on end of narrow ridge.

(8) The local landslide distribution within the Guatemala City area is inconsistent with the detailed seismic-intensity data.

(9) We consider lithology and topography of the steep canyon slopes within the Guatemala City area to be the most important factors determining landslide incidence.

(10) Future strong seismic activity in the Guatemala City area is likely to produce a landslide distribution similar to that from the 1976 earthquake.

REFERENCES CITED

- Bonilla, M. G., 1959, Geological observations in the epicentral area of the San Francisco earthquake of March 22, 1957, in Oakeshott, G. B., ed., *San Francisco earthquakes of March 1957: California Division of Mines Special Report 57*, p. 25-37.
- Bonis, Samuel, Bohnenberger, O. H., and Dengo, Gabriel, 1970, *Mapa Geológico de la Republica de Guatemala (1st ed.)*: Guatemala City, Instituto Geográfico Nacional, scale 1:500,000.
- Castle, R. O., and Youd, T. L., 1972, *Engineering Geology*, in *The Borrego Mountain earthquake of April 9, 1968: U.S. Geological Survey Professional Paper 787*, p. 158-174.
- Espinosa, A. F., Asturias, José, and Quesada, Antonio, 1978, Applying the lessons learned in the 1976 Guatemalan earthquake to earthquake-hazard-zoning problems in Guatemala: *International Symposium on the February 4, 1976 Guatemalan Earthquake and the Reconstruction Process, Guatemala City, 1978, Proceedings*, v. 1, p. 1-91.
- Espinosa, A. F., Husid, Raul, and Quesada, Antonio, 1976, Intensity distribution and source parameters from field observations, in Espinosa, A. F., ed., *The Guatemalan earthquake of February 4, 1976, a preliminary report: U.S. Geological Survey Professional Paper 1002*, p. 52-66.
- Keefer, D. K., 1976, Earthflows in the Coast Ranges of central California: *Preliminary report: U.S. Geological Survey Open-File Report 76-734*, 63 p.

- Keefer, D. K., Wieczorek, G. F., Harp, E. L., and Tuel, D. H., Preliminary assessment of seismically induced landslide susceptibility: International Conference on Microzonation for Safer Construction—Research and Application, 2d, San Francisco, 1978, Proceedings, v. 1, p. 279-290.
- Koch, A. J., and McLean, Hugh, 1975, Pleistocene tephra and ash flow deposits in the volcanic highlands of Guatemala: Geological Society of America Bulletin, v. 86, no. 4, p. 529-541.
- Langer, C. J., Whitcomb, J. P., and Aburto, Q., Arturo, 1976, Aftershocks from local data, in Espinosa, A. F., ed., The Guatemalan earthquake of February 4, 1976, preliminary report: U.S. Geological Survey Professional Paper 1002, p. 30-37.
- Morton, D. M., 1971, Seismically triggered landslides in the area above the San Fernando Valley, in The San Fernando, California, earthquake of February 9, 1971: U.S. Geological Survey Professional Paper 733, p. 99-104.
- Nason, R. D., 1971, Shattered earth at Wallaby Street, Sylmar, in The San Fernando, California, earthquake of February 9, 1971: U.S. Geological Survey Professional Paper 733, p. 97-98.
- Person, Waverly, Spence, William, and Dewey, J. W., 1976, Main event and principal aftershocks from teleseismic data, in Espinosa, A. F., ed., The Guatemalan earthquake of February 4, 1976, preliminary report: U.S. Geological Survey Professional Paper 1002, p. 17-18.
- Plafker, George, Bonilla, M. G., and Bonis, S. B., 1976, Geologic effects, in Espinosa, A. F., ed., The Guatemalan earthquake of February 4, 1976, preliminary report: U.S. Geological Survey Professional Paper 1002, p. 38-51.
- Plafker, George, Erickson, G. E., and Concha, J. F., 1971, Geological aspects of the May 31, 1970, Perú earthquake: Seismological Society of America Bulletin, v. 61, no. 3, p. 543-578.
- Tuthill, S. J., and Laird, W. M., 1966, Geomorphic effects of the earthquake of March 27, 1964, in the Martin-Bering Rivers area, Alaska: U.S. Geological Survey Professional Paper 543-B, p. B1-B29.
- Varnes, D. J., 1978, Slope movement types and processes, chap. 2 of Schuster, R. L., and Krizek, R. S., eds., Landslides: Analysis and control: National Academy of Sciences, Transportation Research Board Special Report 176, p. 11-33.
- Weischet, Wolfgang, 1963, Further observations of geologic and geomorphic changes resulting from the catastrophic earthquake of May 1960, in Chile: Seismological Society of America Bulletin, v. 53, no. 6, p. 1237-1257.
- Wood, H. O., and Neumann, Frank, 1931, Modified Mercalli intensity scale of 1931: Seismological Society of America Bulletin, v. 21, no. 4, p. 277-283.
- Wong, H. L., and Jennings, P. C., 1975, Effects of canyon topography on strong ground motion: Seismological Society of America Bulletin, v. 65, no. 5, p. 1239-1257.
- Wright, Charles, and Mella, Arnaldo, 1963, Modifications to the soil pattern of south-central Chile resulting from seismic and associated phenomena during the period May to August 1960: Seismological Society of America Bulletin, v. 53, no. 6, p. 1367-1402.
- Youd, T. L., and Hoose, S. N., 1977, Historic ground failure in northern California triggered by earthquakes: U.S. Geological Survey Professional Paper 993, 177 p.